



INSTITUTO POLITECNICO NACIONAL
CENTRO INTERDISCIPLINARIO DE CIENCIAS MARINAS



**The Nursery Area of the Devil Ray (*Mobula
munkiana*) at a marine protected area in the
Espíritu Santo Archipelago, Gulf of California,
Mexico**

TESIS

QUE PARA OBTENER EL GRADO DE
MAESTRÍA EN CIENCIAS EN MANEJO DE RECURSOS MARINOS

PRESENTA

MARTA LAURA DÍAZ PALACIOS

LA PAZ, B.C.S, ENERO DE 2019



INSTITUTO POLITÉCNICO NACIONAL
SECRETARIA DE INVESTIGACIÓN Y POSGRADO
ACTA DE REVISIÓN DE TESIS

En la Ciudad de La Paz, B.C.S. siendo las 12:00 horas del día 29 del mes de Noviembre del 2018 se reunieron los miembros de la Comisión Revisora de Tesis designada por el Colegio de Profesores de Estudios de Posgrado e Investigación de CICIMAR para examinar la tesis titulada:

"THE NURSERY AREA OF THE DEVIL RAY (*Mobula munkiana*) AT A MARINE PROTECTED AREA IN THE ESPIRITU SANTO ARCHIPELAGO, GULF OF CALIFORNIA, MEXICO"

Presentada por el alumno:

<u>DIAZ</u>	<u>PALACIOS</u>	<u>MARTA</u>
Apellido paterno	materno	nombre(s)
Con registro: <u>A 1 7 0 5 9 7</u>		

Aspirante de:

MAESTRIA EN CIENCIAS EN MANEJO DE RECURSOS MARINOS

Después de intercambiar opiniones los miembros de la Comisión manifestaron **APROBAR LA DEFENSA DE LA TESIS**, en virtud de que satisface los requisitos señalados por las disposiciones reglamentarias vigentes.

LA COMISION REVISORA

Directores de Tesis

Rogelio G. A.
DR. ROGELIO GONZÁLEZ ARMAS
Director de Tesis

Hoyos Padilla Mauricio
DR. EDGAR MAURICIO HOYOS PADILLA
2º Director de Tesis

[Signature]
DR. FELIPE GALVÁN MAGAÑA

[Signature]
DR. JAIME GÓMEZ GUTIÉRREZ

[Signature]
DR. DONALD ANGUS CROLL

PRESIDENTE DEL COLEGIO DE PROFESORES

[Signature]
DR. SERGIO HERNÁNDEZ TRUJILLO



I.P.N.
CICIMAR
DIRECCIÓN



**INSTITUTO POLITÉCNICO NACIONAL
SECRETARÍA DE INVESTIGACIÓN Y POSGRADO**

CARTA CESIÓN DE DERECHOS

En la Ciudad de La Paz, B.C.S. el día 06 del mes de Diciembre del año 2018

El (la) que suscribe BIÓL. MARTA DIAZ PALACIOS Alumno (a) del Programa
MAESTRÍA EN CIENCIAS EN MANEJO DE RECURSOS MARINOS

con número de registro A170597 adscrito al CENTRO INTERDISCIPLINARIO DE CIENCIAS MARINAS

manifiesta que es autor(a) intelectual del presente trabajo de tesis, bajo la dirección de:

DR. ROGELIO GONZÁLEZ ARMAS y DR. EDGAR MAURICIO HOYOS PADILLA

y cede los derechos del trabajo titulado:

"THE NURSERY AREA OF THE DEVIL RAY (*Mobula munkiana*) AT A MARINE PROTECTED

AREA IN THE ESPIRITU SANTO ARCHIPELAGO, GULF OF CALIFORNIA, MÉXICO"

al Instituto Politécnico Nacional, para su difusión con fines académicos y de investigación.

Los usuarios de la información no deben reproducir el contenido textual, gráficas o datos del trabajo sin el permiso expreso del autor y/o director del trabajo. Éste, puede ser obtenido escribiendo a la siguiente dirección: martad.palacios@gmail.com - rarmas@ipn.mx - amuakua@gmail.com

Si el permiso se otorga, el usuario deberá dar el agradecimiento correspondiente y citar la fuente del mismo.

BIÓL. MARTA DIAZ PALACIOS

Nombre y firma del alumno

Acknowledgements

A Abel Trejo, GRACIAS. Por ser mi amigo y maestro en el maravilloso mundo de las áreas de crianza. Por enseñarme desde sacar sangre, analizar datos, isótopos, estadística, hasta que la comida nivel chef en campo es posible. Este proyecto sin ti no hubiera sido posible.

A Juan y Felipe Cuevas, por capturar todas las cubanitas que la cuota de cada salida exigía y trabajar 18 horas al día si era requerido. Por ayudarnos en todo y compartir con nosotros sus conocimientos, buen humor y amistad.

Al Doc Rogelio González por ser sencillamente el mejor director de tesis que un proyecto como este podría necesitar. Por ayudarme en cada paso del proceso y estar siempre dispuesto y disponible con una sonrisa.

Al Doc Felipe Galván por su ayuda incondicional y hacerme ver que todo es posible.

Ustedes dos son un ejemplo a seguir de cómo ser grandes científicos y mejores personas. Una inspiración para todos sus alumnos.

Al Doc Mauricio Hoyos por abrirme las puertas de Pelagios Kakunjá y haber confiado en mis ideas. Por toda la ayuda y enseñanzas que Pelagios me ha ofrecido a lo largo del camino.

A todos los miembros de Pelagios Kakunjá y del Laboratorio de Tiburones y Rayas de CICIMAR que me ayudaron en mis monitoreos en campo o en el procesamiento de las muestras, en especial a Francesca, Walter, Armando, Miquel, Gádor, Mireia y Frida, gracias por siempre ayudarme con una sonrisa.

A Luis por acompañarme y soportarme durante el último año de muestreo y de tesis, aportándome largas sesiones de olas y ayuda infinita. Gracias.

A Citlali del Valle por ayudarme en el procesamiento y separación de las muestras de zooplankton y por ser una entusiasta de las mobulas.

A los trabajadores de campamento de FUNBAJA y a Enrique por todo su apoyo en la logística durante todo el proyecto, nos facilitaron increíblemente la vida.

Agradezco a los doctores Jaime Gómez-Gutiérrez y a Fernando R. Elorriaga-Verplancken por sus valiosas aportaciones a este trabajo y al manuscrito.

I thank Thomas P. Peschak for planting the seed in my head about this inspiring project.

I am deeply grateful to Don Croll and Kelly Newton for invite me to El Pardito and allow me to learn from the best ones, for trust in me and help me with ideas and financial aid.

I thank Josh Stewart for their overall assistance, advice and help during my master Science project.

I thank Elena Pérez for reviewing the English of the manuscript.

This work was financially supported by Monterey Bay Aquarium, Pelagios Kakunjá, University of California Santa Cruz, Quino el Guardian Liveboards, IdeaWild, Alianza WWF Fundacion Telmex/Telcel and NatGeo.

I thank the Instituto Politécnico Nacional (SIP 20180012, SIP 20170585) and the Comisión Nacional para la Ciencia y Tecnología (CONACYT) of Mexico that supported MDP to carry out this work.

I thank the Comisión Nacional de Acuacultura y Pesca (CONAPESCA) for granting us research permit PPF/DGOPA-133/17, as well as the Comisión Nacional de Areas Naturales Protegidas (CONANP) - Islas del Golfo/Parque Nacional Zona Marina del Archipiélago Espiritu Santo, for field work authorization and support.

Y por último pero no menos importante, a mi familia querida por siempre apoyarme, dejarme ser y darme alas para creer que con esfuerzo y determinación nada es imposible en esta vida.

Table of Contents

Acknowledgements.....	i
Table of contents.....	iii
List of tables.....	iv
List of figures.....	iv
Abstract.....	1
Introduction.....	3
Methods.....	5
Study site.....	5
Captures and Conventional tagging.....	6
Acoustic Telemetry.....	6
Enviromental factors.....	7
Stable isotope Analysis.....	8
Statistic Analysis.....	9
Captures and Conventional tagging.....	9
Acoustic Telemetry.....	9
Enviromental factors.....	11
Stable isotope Analysis	11
Results.....	13
Captures and conventional tagging.....	13
Acoustic Telemetry.....	17
Enviromental factors.....	22
Stable isotope Analysis.....	24
Discusion.....	28
Nursery Area.....	28
Segregation by Size and Sex and Mating Season.....	29
Pupping Season.....	31
Habitat Use of Neonates and Juveniles.....	32
Conclusions.....	34
References.....	36

List of tables

Table 1. Release and recapture details for tagged Munk's devil rays. **Ind** is the number of the tag of the individual. **DW** (cm) is the disc width of the individual. **GR** (cm) is the growth rate, difference between DW at recapture and DW at tagging. **DL** are the days at liberty of the individual from the day it was tagged until its recapture. **TD** (Km) is the travelled distance.....17

Table 2. Passive acoustic details for tagged Munk's devil ray. TDATE is the tagging date. Loc is the tagging location N Days is the total number of days with a detection anywhere within the array. MCD is the maximum number of consecutive days the individual was detected at EG. DUR is the duration between date of tagging and the last day detected. N Hits is the total number of detections for each individual. MLD is the minimum linear dispersal distance between two furthest receivers with detections (Km). RI ESA is the residency index for the entire array around ESA.19

Table 3. Stable isotopes summary information for blood tissue collected from *M. munkiana* during 2017-2018 at ESA. All values are means \pm SD.....25

Table 4. Stable isotopes summary for zooplankton samples collected during the cold season 2017-2018. All values are means \pm SD. *Mean trophic fractionation between Munk's devil rays and the mean value for each zooplankton taxonomic group.....27

List of figures

Figure 1. Study site location. Red dots indicate acoustic receivers.....5

Figure 2. Disc width frequency distributions of tagged Munk's devil rays collected at the EG from August 2017 to June 2018. The disk width of first maturity was 97 cm for females and 98 cm for males (showed in dotted pink and blue lines).....13

Figure 3. A) Map of EG with the locations where Munk’s devil rays of various life stages were captured during our sampling period. B) Seasonal frequency distribution of Munk’s devil ray captured per maturity stage at EG (ESA).....15

Figure 4. A) Juvenile male Munk’s devil ray with undeveloped claspers (pointed with an arrow) collected at EG during August 2017. B) Adult female Munk’s devil ray with a distended cloaca collected during April 2018. C) A pregnant female with a traditional tag at EG collected in June 2018. D) Neonate with the scar of the umbilical cord (indicated by an arrow) in August 2017.....16

Figure 5. Residency index (RI) of Munk’s devil rays tagged at EG with internal acoustic transmitters. RI is given for each receiver station (RS) located around the ESA. Individual devil rays (Number #Sex-DW in cm) are arranged by increasing disk width from top to bottom..... 18

Figure 6. Timeline showing the days each individual Munk’s devil ray was detected in the ESA, from August 2017 to June 2018 with the specific location of each detection color coded. Solid red line indicates mean daily water temperature at EG. Individual devil rays (Number #Sex-DW in cm) are arranged by increasing body size from top to bottom.....20

Figure 7. A) Satellite image of EG. Red dots indicated receiver stations, RS1 shallow receiver (5 m depth) and RS2 deeper receiver (26 m depth). Yellow lines represent the zooplankton sampling stations, RS1, RS2 and coastal station (CS). B) Mean zooplankton biomass abundance per sampling station at EG during day and night time. Standard error are represented in black lines. C) Circular plots showing hours of detections for all Munk’s devil rays (n= 7) at the two receivers of EG. A significant non-uniform distribution of the detections was registered for both receivers ($p < 0.05$).....21

Figure 8. Relationship between the mean monthly residency index (RI) and the daily sea water temperature recorded at EG during each month ($S = 2.496e^9$, p

$< 2.2e^{-16}$, $\rho=0.643$). Higher water temperatures resulted in higher residency index for juveniles and neonates Munk's devil ray.....22

Figure 9. Mean monthly residency index at EG for all Munk's devil rays (n=7). The vertical lines represent the standard error (SE) for each month's residency index. Red line is the mean monthly temperature at EG and green dots are the mean monthly zooplankton biovolume.....24

Figure 10. $\delta^{15}\text{N}$ and $\delta^{13}\text{C}$ values for *M. munkiana* during cold (blue) and warm (red) season at ESA during 2017-2018. Points represent the $\delta^{13}\text{C}$ and $\delta^{15}\text{N}$ blood values from each individual. Disc width at which females (97 cm) and males (98 cm) attain adulthood is shown with dotted pink and blue lines, respectively.....25

Figure 11. A) Isotopic values for $\delta^{13}\text{C}$ and $\delta^{15}\text{N}$ from Munk's devil ray blood, preys and zooplankton collected during the cold season at the EG, ESA and Bahía de La Paz area. Points are mean values and dotted lines are the standard deviation for each group. B) Isotopic niche overlapped among *M. munkiana* maturity stages. Points represent the $\delta^{13}\text{C}$ and $\delta^{15}\text{N}$ blood values from each individual. Standard ellipses were calculated using Bayesian statistics with the SIBER analysis.....26

Figure 12. Juvenile Munk's devil ray feeding at night in EG during recreational night dives. A) November 2013; B) October 2014; C) October 2016. Undeveloped claspers are indicated with arrows. Photograph copyrights: A and B. Erick Higera; C. Luke Inman.....29

Abstract

Nursery areas are crucial for elasmobranch populations, where females give birth and, neonates and juveniles spend their first months or years. An ecotourism industry based on the observation of small individuals of Munk's devil ray (*Mobula munkiana*) was established in 2013 in a shallow bay at the Espiritu Santo Archipelago (ESA), Baja California Sur, Mexico. We assess the potential use of this bay as a nursery area of the filter feeder elasmobranch *M. munkiana*. We examine spatial use of the bay during one year in relation to seasonal environmental patterns using a combination of nonlethal methodologies such as traditional tagging (n=95), passive acoustic telemetry (n=7) and stable isotopes analysis (n=69).

Neonates and juveniles comprised 86% of the 95 individuals captured during the study period. The residency index (RI) for tagged neonates and juveniles was significantly higher inside the bay than adjacent offshore habitats ($W_{26}= 182$, $p=0.0001$) with a maximum of 145 consecutive days of residence within the bay. Residency index values were greater during August, September and December; corresponding to the seasonal peak in water temperature and zooplankton biovolumen.

The observation of near-term pregnant females, mating behavior, females with distended cloacas and neonates evidenced that the pupping period for this species in this region extends from April to June.

Review of archival photographs and videos obtained from recreational divers and ecotourism agencies operating in the area confirm that the patterns observed during the study period (2017-2018) reflected similar use of the ESA by neonates and juveniles over several years. We emphasize the ecological importance of shallow bays of the ESA for the early life stages of *M. munkiana* and we hypothesize that other nearshore regions in the Gulf of California likely serve as mating, pupping and nursery areas. Therefore, we highlight the need for special consideration for protection of these areas from anthropogenic activities (development, fishing, disturbance).

Resumen

Las áreas de crianza son cruciales para muchas poblaciones de elasmobranquios, dónde las hembras dan a luz y los neonatos y juveniles pasan sus primeros meses o años de vida. En una bahía somera en el Archipiélago de Espíritu Santo (AES) en la península de Baja California, México se estableció desde 2013 una actividad ecoturística de la observación de pequeños individuos de mobulas de Munk (*Mobula munkiana*). Este estudio evalúa el uso potencial de esta bahía como área de crianza para el elasmobranquio filtrador, *M. munkiana*. Se examinó el uso de hábitat durante un año en función de los patrones ambientales mediante métodos no letales como el marcaje tradicional (n=95), la telemetría acústica pasiva (n=7) y el análisis de isótopos estables (n=69).

Neonatos y juveniles tuvieron mayor abundancia representando el 86% de los 95 individuos capturados durante el período de estudio. El índice de residencia (IR) de neonatos y juveniles marcados fue significativamente más alto dentro de la bahía que en los hábitats pelágicos próximos ($W_{26} = 182, p = 0.0001$) con un máximo de 145 días consecutivos de residencia dentro de la bahía. El mayor IR de neonatos y juveniles se observó durante agosto, septiembre y diciembre coincidiendo con los picos estacionales de temperatura y biovolumen de zooplancton.

La presencia de hembras embarazadas, observación de comportamiento de cortejo, hembras con cloacas distendidas y neonatos evidenció un periodo de reproducción de abril a junio. Reportes de neonatos y juveniles durante varios años confirmados mediante fotografías y videos de buzos de las agencias de ecoturismo que operan en el área indican el uso repetido de *M. munkiana* en el AES. Por lo que destacamos la importancia ecológica que las bahías someras del AES juegan en los primeros estadios de vida de *M. munkiana* y sugerimos que otras áreas costeras en el Golfo de California pueden estar funcionando como áreas de apareamiento, alumbramiento y crianza. Por ello se ha de tomar especial consideración en estas regiones a las actividades antrópicas (pesca, desarrollos turísticos y alteraciones del medio).

INTRODUCTION

Nursery areas are crucial for many elasmobranch populations (Heupel *et al.*, 2007). These discrete areas have been shown to have biotic and abiotic features important for pupping and enhancing the survival of neonates, young of the year (YOY) and juveniles (Castro, 1993; Heupel & Simpfendorfer, 2011). Elasmobranch nursery areas must follow at least three criteria as proposed for sharks (Heupel *et al.*, 2007) and batoids (Martins *et al.*, 2018): 1) neonates, YOY, and juveniles are more commonly encountered than in other adjacent areas, 2) individuals tend to remain or return to the area over weeks or months, and 3) the area is used in a similar manner repeatedly across years.

While many studies have identified the importance of nursery areas for sharks (Snelson *et al.*, 1984; Simpfendorfer & Milward, 1993; Compagno *et al.*, 1995; Heupel & Simpfendorfer, 2002; Heupel *et al.*, 2007) little is known about nursery areas for batoids (Cerutti-Pereyra *et al.*, 2004; Yokota & Lessa, 2006; Stewart *et al.*, 2018a). Indeed, only one study had identified a nursery area for Mobulids (*Mobula birostris* and *M. cf. birostris*) in the Gulf of Mexico (Stewart *et al.*, 2018a). Mobulids are planktivorous filter feeders with vulnerable life histories (Couturier *et al.*, 2012, Stewart *et al.*, 2018b) that include the lowest fecundity of all elasmobranchs (litter size of one pup) (Dulvy *et al.*, 2014), and delayed, ovoviviparous matrotrophic reproduction cycles of 1-3 years (Notarbartolo-di-Sciara, 1988; Compagno & Last, 1999; Marshall & Bennett, 2010; Wourms, 1977; Dulvy & Reynolds, 1997; Croll *et al.*, 2016), with a litter size of one pup (Hoenig & Gruber, 1990; Stevens *et al.*, 2000).

Such low reproductive rates make mobulids extremely vulnerable to anthropogenic impacts including targeted small-scale fisheries (Notarbartolo-di-Sciara, 1988; White *et al.*, 2006; Rohner *et al.*, 2013) and bycatch in small- and large-scale fisheries (Paulin *et al.*, 1982; White *et al.*, 2006). As a result, all evaluated mobulid species are IUCN threatened or near-threatened, with many species experiencing population declines (Alaba *et al.*, 2002, Ward-Paige *et al.*, 2013; White *et al.*, 2015). Despite its vulnerability, existing studies have mainly focused on the taxonomy, movements, feeding habits and reproduction behaviour (Notarbartolo di Sciara, 1988; Sampson *et al.*, 2010; Croll *et al.*, 2012; Mendonça *et al.*, 2018, Stewart *et al.*, 2017; Duffy *et al.*, 2017) of adults, with little information on the ecology and behavior of early life stages.

Munk's devil ray (*Mobula munkiana*) is endemic to the Eastern Pacific, with a range that extends from the Gulf of California, Mexico to Peru and it is typically found in neritic and coastal habitats (Bizarro *et al.*, 2006). It is currently classified as "Near Threatened" on the International Union for the Conservation of Nature (IUCN) Red List assessment (Bizarro *et al.*, 2006) and is nationally protected in Mexican waters under the NOM-029-PESC-2006 and NOM-059-SEMARNAT-2018 regulation. However illegal fishing still exists in several areas of the Gulf of California (Heinrichs *et al.*, 2011). Munk's devil ray has an estimated disk width at birth of 35 cm and reaches up to 110 cm as adult (Notarbartolo di Sciara, 1987; Lopez, 2009) and is particularly known for its social behavior (Notarbartolo di Sciara, 1988; Bizarro *et al.*, 2006); often congregating in large aggregations of thousands of individuals, presumedly for mating purposes (Stewart *et al.*, 2018b). When Notarbartolo-Di-Sciara, (1987) described the species in the Southern Gulf of California he found that individuals segregated by size (Notarbartolo di Sciara, 1987, 1988; Smith *et al.*, 2009), leading to the potential for differential habitat use between juvenile and adult stages.

Since 2013, local fishermen and tour operators in the Southern Gulf of California, have known a well-established aggregation of devil rays in the shallow bay with sandy bottom seafloor of Ensenada Grande (EG) located on the northwest part of the Espiritu Santo Archipelago (ESA). In recent years, an ecotourism activity has developed on this knowledge bringing recreational divers to observe feeding aggregations of neonates and juveniles of Munk's devil rays attracted to the zooplankton artificially concentrated with lights during certain months of the year. These anecdotal observations provided the opportunity to examine whether mobulid rays utilize nursery areas for mating, pupping and foraging of juveniles.

We investigate if *M. munkiana* uses the shallow EG as a nursery area, following the criteria proposed by Heuple *et al.* (2007) and Martins *et al.* (2018). We use a combination of nonlethal methodologies including traditional tagging, passive acoustic telemetry, stable isotopes analysis, and biooceanographic sampling to examine spatial use and foraging ecology of early life history stage *M. munkiana*.

We emphasize the ecological significance of shallow coastal bays of the ESA and the surrounding region on the early life stages of *M. munkiana*. This biological information is relevant for protection managing and attempts to decrease bycatch of *M. munkiana* in coastal artisanal fisheries in the region. The present study is a baseline for the management of the ecotourism activity carried out in the ESA.

METHODS

Study site

ESA, located on the west south part of the Gulf of California is the oriental limit of Bahía de La Paz (**Fig. 1**). ESA was declared a Marine National Park in 2007 and allows artisanal fisheries and ecotourism activities in some restricted areas. The bathymetry of the oriental coast of ESA has stepped slopes falling up to 100 m just a few meters from the shore. Our main study area EG, is located on the west coast of ESA and is comprised of several sandy bottom embayments (< 40 m depth) with small slopes (Gaitan *et al.*, 2005).

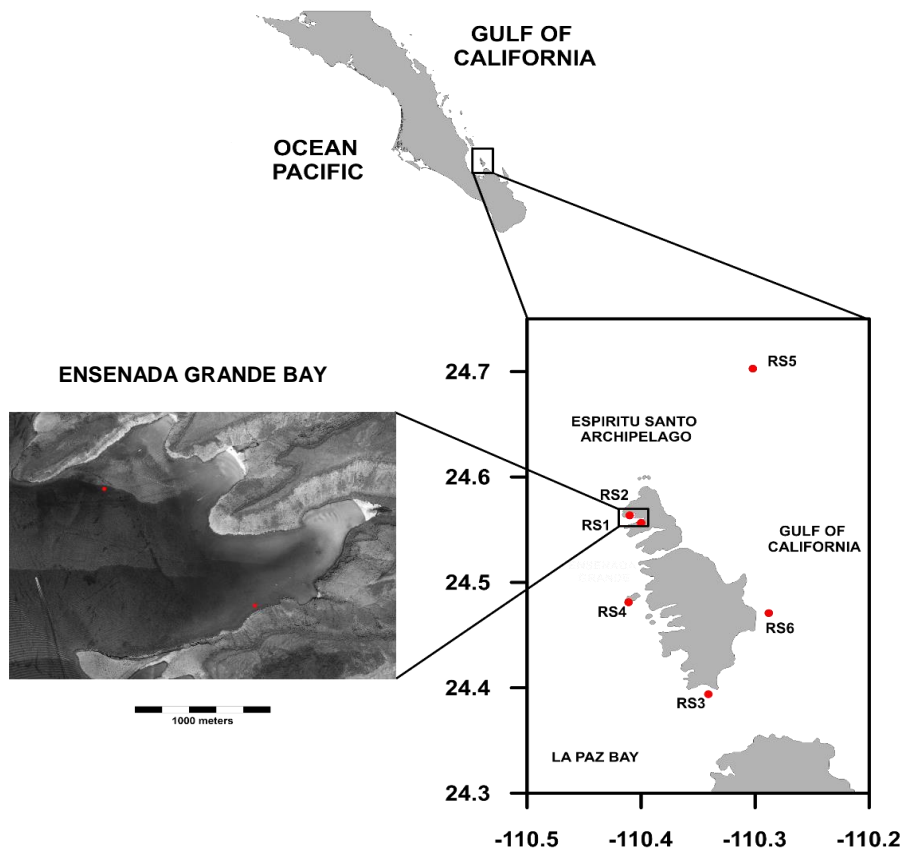


Figure 1. Study site location. Red dots indicate acoustic receivers.

This archipelago is influenced by the monsoonal wind pattern of the Gulf of California with northwesterly winds that cause weak upwelling events during the cold season (December to May) with primary production rates ranging between 1.16–1.91 g C m² d⁻¹ (Hidalgo-Gonzalez & Alvarez-Borrego, 2004). Strong thermal stratification occurs during the warm season (June to November), when the peninsular coast of Baja California peninsula does not present strong upwelling (Santamaria del Angel *et al.*, 1999) with low primary production rates ranging 0.39 to 0.49 g C m² d⁻¹ (Hidalgo-Gonzalez & Alvarez-Borrego, 2004).

Captures and Conventional Tagging

Munk's devil rays were caught between August 2017 and June 2018 at EG during 5 capture trips of three-days duration each one. Individuals were captured with encircling surface cotton twine nets 150 m long, 15 m deep, with 25 cm mesh net. Once captured, we maintained the individuals inside the water, allowing water to pass over their gills to reduce stress levels before transferring them into a holding tank on the boat. Individuals were sexed, measured for total length (TL) and disc width (DW), recording mating scars on pectoral fins and cloaca state of females and development state of claspers of males. Genetic and blood samples were taken, and individuals were tagged with conventional fish tags (FLOY TAG, Inc.) in the dorsal part of the pectoral fin for identification purposes. The capture-to-release was typically completed in <5 min and all devil rays were released in good conditions.

Individuals with umbilical scar were classified as neonates. Munk's devil ray maturity was classified according to estimates of size at maturity as juvenile (<97-98 cm DW) or adult (> 97-98 cm DW) (Lopez, 2009). Pregnant females were classified if showed evidence of a noticeably distended abdominal region on both the dorsal and ventral surfaces as defined by *Mobula birostris* (Marshall & Bennett, 2010).

Acoustic Telemetry

Four neonates and three juveniles Munk's devil rays were captured on August 2017 at EG and fitted with internal acoustic transmitters (Vemco V13; Vemco Ltd, Nova Scotia, Canada) with an expected battery life of 991 days. Transmitters operated on 69 kHz and were coded to pulse randomly once every 40–80 s

allowing the simultaneous monitoring of multiple individuals without continuous signal overlap. Transmitters were coated with beeswax to avoid infections and surgically inserted into the abdominal cavity doing a 5 cm incision. The incision was closed with synthetic surgical sutures. All devil rays were released without mortality and in good conditions. The tagging and surgical procedures followed the Institutional Animal Care and Use Committee of the University of California, Davis (IACUC, Protocol No. 16022).

Six acoustic receivers (VR2w and VR2Tx, Vemco, Ltd, Nova Scotia, Canada) were deployed at the ESA as part of 17 tracking array installed at Bahía de La Paz to passively track the movement of neonate and juvenile Munk's devil rays between August 2017–September 2018. Receivers were moored at depths between 5–26 m at locations previously known to be frequented by Munk's devil rays at the ESA. The receiver array covered EG (RS1 at 5 m and RS2 at 26 m depth). Receiver RS3 was placed 1 km away from the coast at the San Lorenzo channel that connects Bahía de La Paz to the Gulf of California south of the ESA. RS4 was placed on the limit of the continental shelf west of the Ballena Island and RS5 was placed on a seamount about 18 km northwest from the ESA.

Range testing showed the maximum detection range for receivers at the ESA was 350 m. Receivers recorded the identity, time and date of the Munk's devil rays tagged that swam within the detection range of the receivers. Receivers from Bahía de La Paz form part of a large research network program with array of listening stations deployed through the Eastern Tropical Pacific (migramar.org).

Enviromental factors

Temperature loggers (HOBO 64k Pendant; accuracy: $\pm 0.53^{\circ}\text{C}$ from $0\text{--}50^{\circ}\text{C}$, range: -20 to 50°C) were attached to the receivers in the EG recording every 2 h during the study period. Zooplankton was sampled during day and night at three locations inside EG. Two of these stations were located close to RS1 and RS2 receivers. A total of 125 zooplankton samples were collected from August 2017 to June 2018 (25 samples per monitored month). Zooplankton was collected during three min oblique tows of a 60-cm mouth diameter zooplankton net (300 μm mesh) equipped with a calibrated flow meter (G.O. 2030R) mounted in the mouth of the net to estimate the filtered seawater volume. Samples were preserved with 4% formalin. Zooplankton biomass volume was estimated for

each sample using the displacement volume method (Smith & Richardson, 1979).

Stable Isotope Analysis

Samples of whole blood (“blood” hereafter) of 69 Munk’s devil ray were collected (Warm season 2017: 9 neonates, 18 juveniles, 9 adults; Cold season 2018: 26 juveniles; 5 adults, 2 pregnant adults). Samples of 3 ml of blood were extracted with a 5 ml gauge sterile needle from the dorsal side of the left pectoral fin storing in Heparin K2 EDTA tubes (BD Vacutainer), placed on ice and posteriorly at land frozen. Lipid extraction was not necessary due to the low molar C:N ratios in the Munk’s devil rays blood samples (2.4 ± 0.11 , mean \pm SD), which indicates low lipid concentrations in the tissues and low variability among individuals (Post *et al.*, 2007).

Zooplankton samples for stable isotope were collected during the cold season of 2018 at EG and around the ESA and Bahía de La Paz. Zooplankton samples were collected with the same net but towed near the surface during 15 min. The zooplankton samples were immediately frozen. Euphausiids, mysis and copepods collected at EG during April 2018 were sorted out from the zooplankton samples to measure stable isotopes and compare with the isotopic signal of *M. munkiana*.

Several authors suggest that dietary lipids in prey may be routed directly to consumers tissues, therefore they should be left on prey samples to be taken into consideration to characterize the diet of the consumers (Newsome *et al.*, 2010a, Newsome *et al.*, 2010b, Parng *et al.*, 2014). For this reason, we did not lipid-extract in prey samples although C:N values (5.4 ± 0.7 , mean \pm SD) indicated they were lipid-rich as defined by Newsome *et al.* (2010).

Tissue turn over rate of blood was calculated using the mean values from serum and blood red cells (Caut *et al.*, 2013) assuming a similar tissue turnover rate of 87 days estimated for the shark *Rhizoprionodon longurio* (Trejo, 2017).

All blood samples were dried for 48 h via freeze-drying using a FreeZone 2.5 (LABCONCO Ltd.), and then grounded into a fine powder with a mortar and pestle. Subsamples of 0.07- 0.09 mg, were weighed and packed in 8x5 mm tin cups.

The $\delta^{13}\text{C}$ and $\delta^{15}\text{N}$ values of blood tissue and prey samples were determined with a carbon-nitrogen analyzer coupled with an isotope ratio mass spectrometer

Delta V Plus (Thermo Scientific). Isotope values are reported as δ -values (as ‰) relative to Vienna PeeDee Belemnite (VPDB) and atmospheric N₂ standards for carbon and nitrogen. Analytical precision was 0.2 ‰ estimated from standards analyzed with the samples.

Statistic Analysis

Data analyses for this study were conducted in the R environment (R Development Core Team, 2018).

Captures and Conventional Tagging

We used the data collected from captures and conventional tagging to characterize the Munk's devil ray size and demographic composition of the population at EG. To estimate if there is a bias in the sex proportion of juveniles and neonates I did an X^2 test. A Wilcoxon tests was done to compare disk width and sex distribution because the size and sex frequency distribution did not follow a normal distribution ($W_{94} = 0.925, p < 0.05$). Capture locations were plotted using SURFER (Golden Software, Inc., 2011) and the coast line data was extracted from GEODAS-NG (National Geophysical Data Center, 2000). The minimum distance between capture and recapture sites was calculated avoiding land with the route tool in Google Earth PRO. An X^2 was calculated to compare disk width distribution of recaptured devil rays (at tagging) and disk width distribution of all captured devil rays to identify potential bias in the recaptures. Pearson's correlation coefficients were estimated between distance traveled and size of devil ray at recapture. A t-test was used to test for differences in average distance traveled between sexes and maturity stage.

Acoustic Telemetry

Data collected from acoustic receivers were analyzed to examine presence, residency time and movement patterns of the Munk's devil ray population around the ESA. We filtered the data and used only the detections with two or more consecutive detections to avoid potentially false detections that arise from signal collisions or background noise (VUE software Manual version 2.5).

Residency

Residency of each individual for the ESA was calculated dividing the number of days a Munk's devil ray was detected with at least two detections within a single day, on any receiver within the array between the number of days since the animal was tagged until the receivers were taken out of the water. A value of one indicated an individual was always present, while zero indicated an individual was not detected after release. Residency index for each receiver on the array was also calculated. Daily presence data were analyzed to determine the number of consecutive days that an individual was resident (continuous presence). A Spearman correlation was performed between the Munk's devil ray disk width and the residency index at the ESA. A t-test was then used to compare the influence of maturity stage and sex on the ESA residency index for each individual.

Habitat preference

Habitat preference was studied by grouping the acoustic receivers on inside-bay receivers (EG with RS1 and RS2) and offshore receivers (RS3, RS4, RS5, and RS6). A Wilcoxon test was used to compare the residency index found on inside-bay receivers and offshore receivers.

Seasonality

To analyze the months of the year when the Munk's devil ray was more resident at EG during the monitoring period, we applied a Kruskal-Wallis non-parametric test to the residency index across months. A post-hoc Dunn test analysis was done to test significant difference among months.

Daily detection of rays

To quantify diel changes in the Munk's devil ray presence of EG we did circular plots of the number of detections per hours of daytime (6 am- 19 pm) and nighttime (19 pm- 6 am); diel times were determined using defined cutoffs for dawn and dusk (McCauley *et al.*, 2014) We used Rao's test to analyze the uniformity of the detections for the RS1 and RS2 receivers.

Movements

The Munk's devil ray movements were visualized by plotting presence and daily mean temperature data, gathered from all the receivers in the array and the EG temperature logger during the monitoring period. We calculated the "minimum linear dispersal distance" MLD for each individual defined as the distance between the two furthest receivers at which an individual was ever detected. We used the route tool in Google Earth PRO to calculate the MLD.

Environmental factors

A Wilcoxon test was used to compare seawater temperatures among seasons because data followed a non-normal frequency distribution ($W_{3473} = 0.88501$, $p < 2.2e-16$). We tested the correlation between the seawater temperature and the mean monthly residency index at EG using a Spearman correlation. Wilcoxon test was used to compare zooplankton biovolume between day/ night and between warm/ cold seasons because also this variable had non-normal distribution. Kruskal-Wallis non-parametric test was done to compare the zooplankton biovolume among months among sampling stations. Post-hoc Dunn test analysis was done to determine which months and sampling station significantly differ from each other. We tested the correlation between the zooplankton biovolume and the mean monthly residency index at EG using a Spearman correlation.

Stable Isotopes Analysis

Devil Rays

A Wilcoxon test was used to compare isotopic values among seasons and sexes because $\delta^{15}\text{N}$ and $\delta^{13}\text{C}$ values had no normal frequency distribution. Kruskal-Wallis non-parametric test was performed to compare isotopic values among devil ray maturity stages.

Isotopic niche areas

The niche breadth and trophic overlap of each Munk's devil ray maturity stage was inferred using the Stable Isotope Bayesian Ellipses in R (SIBER) package (Jackson *et al.*, 2011). This statistical method creates standard ellipses using a covariance matrix defining their shape and area in a bivariate $\delta^{15}\text{N}$ and $\delta^{13}\text{C}$ space. Niche breadth is represented by the standard ellipse corrected area (SEAc). Trophic overlap was calculated using SEAc and the ellipse overlap value

where values close to 1 represent a high degree of trophic overlap among individuals of distinct maturity stages.

Trophic position

The trophic position (TP) of each Munk's devil ray individual in the food web was calculated using the $\delta^{15}\text{N}$ value with equation proposed by Post (2002):

$$TP_{\text{Elasmobranch}} = (\delta^{15}\text{N}_{\text{Elasmobranch}} - \delta^{15}\text{N}_{\text{Baseline}}) / (\Delta^{15}\text{N}_{\text{Elasmobranch}}) + TP_{\text{Baseline}}$$

The mean value of $\delta^{15}\text{N}$ 13.90 ‰, was estimated from the zooplankton samples collected during the cold season at EG, as $\delta^{15}\text{N}$ baseline. Due to the high variability of the $\delta^{15}\text{N}$ and $\delta^{13}\text{C}$ values in phytoplankton, primary consumers are typically used as the baseline (Cabana & Rasmussen, 1996; Vander-Zanden & Rasmussen, 2001). The mean $\Delta \delta^{15}\text{N}$ values from serum and red blood cells reported by Kim *et al.* (2012) was used to calculate the trophic discrimination factor from blood tissue in *M. munkiana* same as calculated by Trejo (2017) with a mean value of $2.3 \pm 0.6\text{‰}$ (mean \pm SD) $\Delta \delta^{15}\text{N}$ for whole blood in sharks. Trophic position from the baseline, the zooplankton, was 2 (Post *et al.*, 2000). A Wilcoxon test was done to compare trophic position between seasons and a Kruskal-Wallis non-parametric test was done to compare trophic position among maturity stages.

Zooplankton

An ANOVA one-way test was performed to compare isotopic differences among prey taxonomic groups (euphausiids, mysids and copepods). A Kruskal-Wallis non-parametric test was used to compare isotopic variability among areas because the isotopic values of zooplankton samples (all taxonomic groups) collected at different areas did not follow a normal distribution.

Trophic fraction

We calculate the discrimination trophic factor using the following Hussey *et al.* (2010) equation:

$$\Delta hX = \delta hX_{\text{Consumer}} - \delta hX_{\text{Prey}}$$

where ΔhX is the trophic factor, h is the heavy isotope and X is the element. To obtain the differences in the isotopic composition among Munk's devil rays and its preys we calculate the trophic factor for each devil ray individual with the mean value for each zooplankton taxonomic group (euphausiids, mysids and copepods).

RESULTS

Captures and Conventional Tagging

A total of 95 Munk's devil rays were captured at EG from August 2017 to June 2018 during five capture periods. Juveniles (65%) and neonates (19%) dominated the sampled population with a sex proportion 1:1 M: F ($X^2= 0.05$, $p > 0.05$).

Munk's devil ray catches and life stage varied seasonally. Neonates were captured only during August and juveniles were present throughout the year. Adults (15%) and pregnant females (1%) were observed April and June. The disk width was not normally distributed (**Fig. 2**) ($W_{94}= 0.925$, $p<0.05$). We found no significant difference in size by sex ($W_{93}=905$, $p > 0.05$).

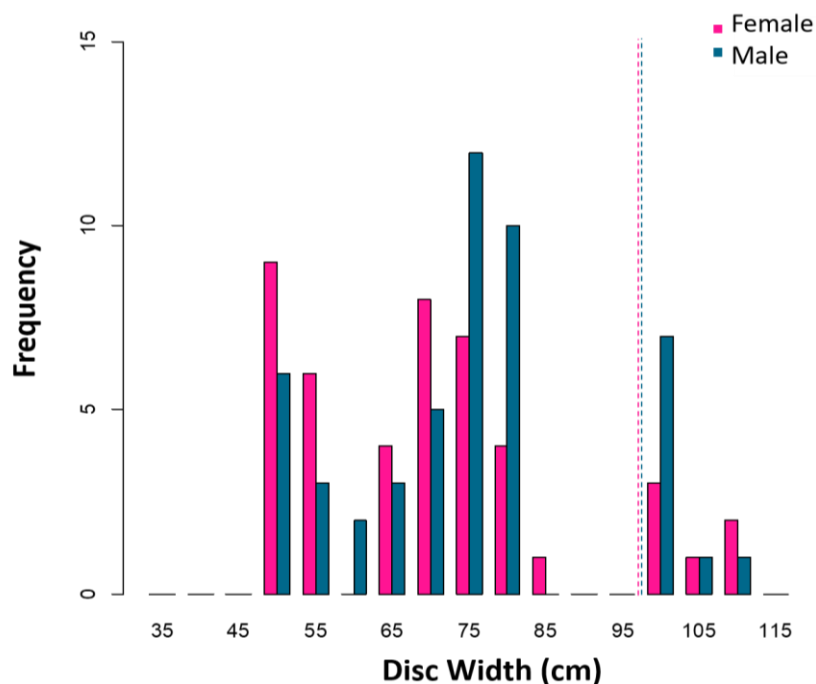
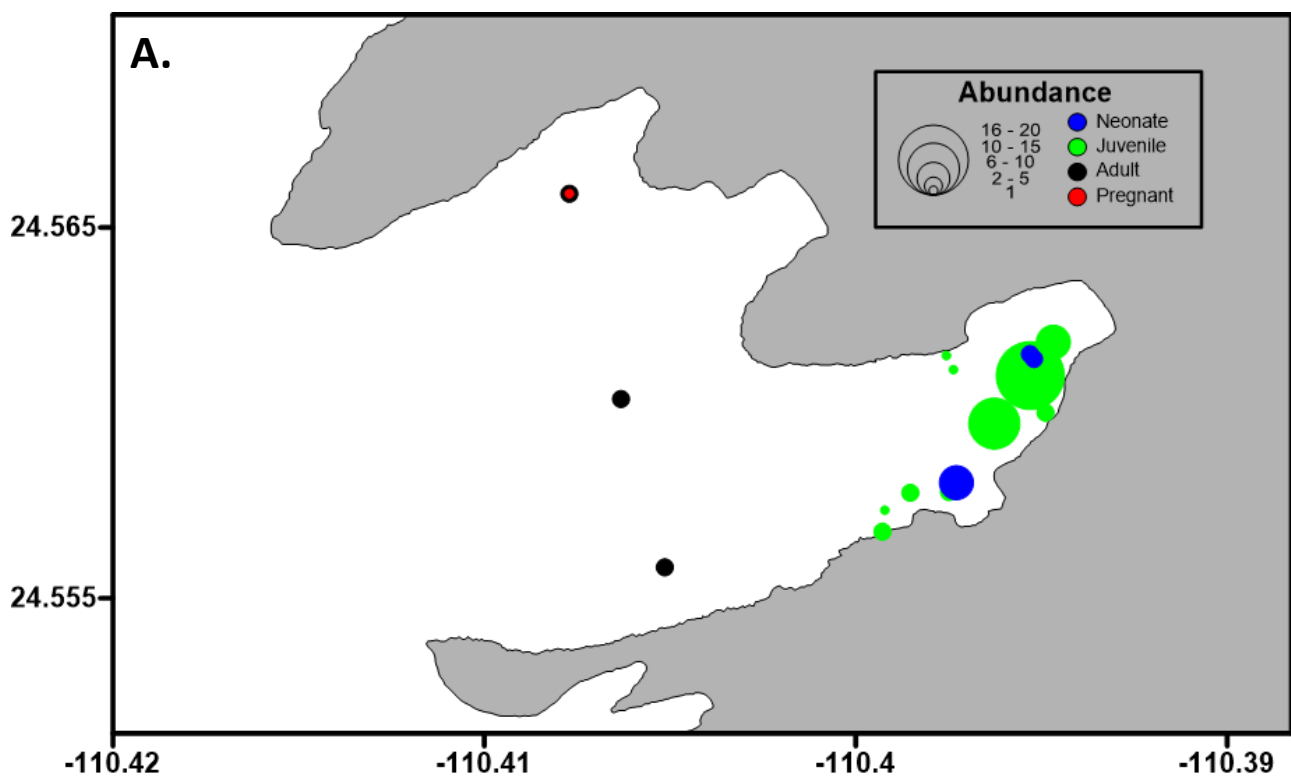


Figure 2. Disc width frequency distributions of tagged Munk's devil rays collected at the EG from August 2017 to June 2018. The disk width of first maturity was 97 cm for females and 98 cm for males (showed in dotted pink and blue lines).

Neonates were identified by the presence on the ventral part below the gills of the umbilical cord scar (**Fig. 4D**). The 18 neonate individuals with an umbilical scar had a disk width range between 49.5–56 cm. Animals within this range of disk width that did not showed evidence of umbilical scars were classified as juveniles. All neonate individuals were caught approximately at noon (12:00 pm) at depths between 2–5 m inside EG during August. We captured up to 7 individuals per catch, but the average number of animals in a school was 4.5 ± 1.73 (mean \pm SD). In these schools only neonates were present.

Juveniles (n=62) had a disk width range of 49-85 cm and were captured in larger schools than neonates with up to 19 individuals and an average of 5.9 ± 6.3 (mean \pm SD) per school. Juveniles were mostly captured at sunset (19:00) during August, October and December. However, when adults were present (April and June) juveniles were captured at noon. Juveniles were not caught with any other life stage individuals indicating size segregation of the schools. Captures were carried out at depths between 2 to 10 m inside EG.

All neonate and juvenile males observed had undeveloped claspers with no rotation (**Fig. 4A**). Neonate and juvenile females showed no evidence of mating scars and the state of the cloaca was normal.



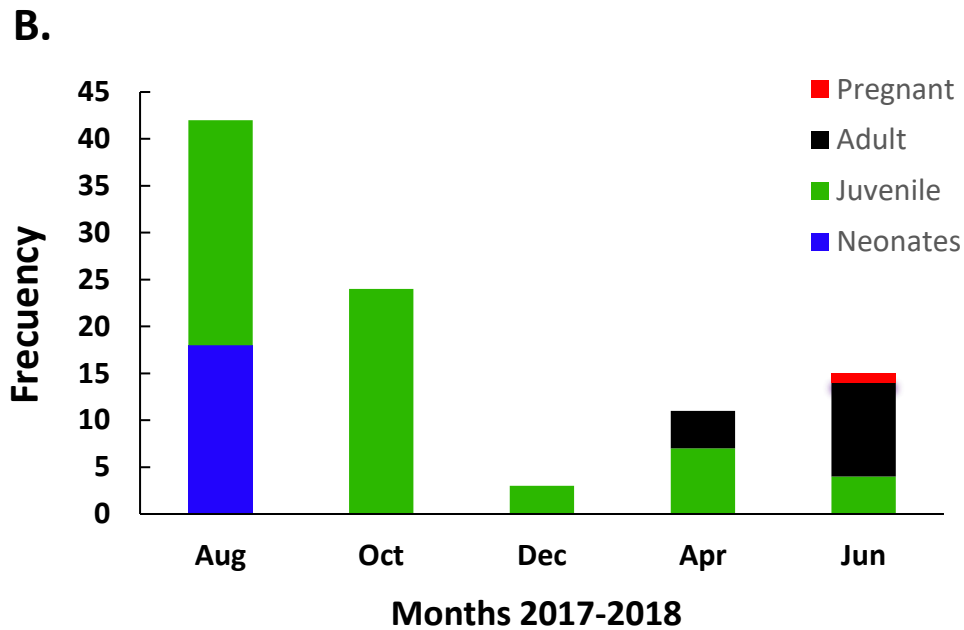


Figure 3. A) Map of EG with the locations where Munk's devil rays of various life stages were captured during our sampling period. **B)** Seasonal frequency distribution of Munk's devil ray captured per maturity stage at EG (ESA).

All adults were captured during afternoon (after 17:00) and were only captured in spring and early summer (April and June). The four adults captured in April 2018 were females with swollen distended cloaca evidenced with a reddish coloration indicating recent parturitions (**Fig. 4B**). During June 2018 was captured a group of one adult female and four adult males showing courtship behavior at surface, initiation and endurance as described for *M. birostris* and *M. alfredi* (Stevens *et al.*, 2018). All these males had developed claspers with semen. Courtship behavior was also observed during April. A female in an advanced state of pregnancy was captured at EG during June 2018 showing distended abdominal region on both the dorsal and ventral surface (**Fig. 4C**). Another pregnant female Munk's devil ray captured in April at ESA exhibited the same morphological characteristics, which was corroborated using a WEED-2000AV portatil ultrasound (Ramirez *et al.* in prep).

The influence of ontogeny on Munk's devil ray spatial distribution was evident during our sampling period. Adults were only captured in >15 m depths while neonates and juveniles were captured in depths between 2 and 10 m.

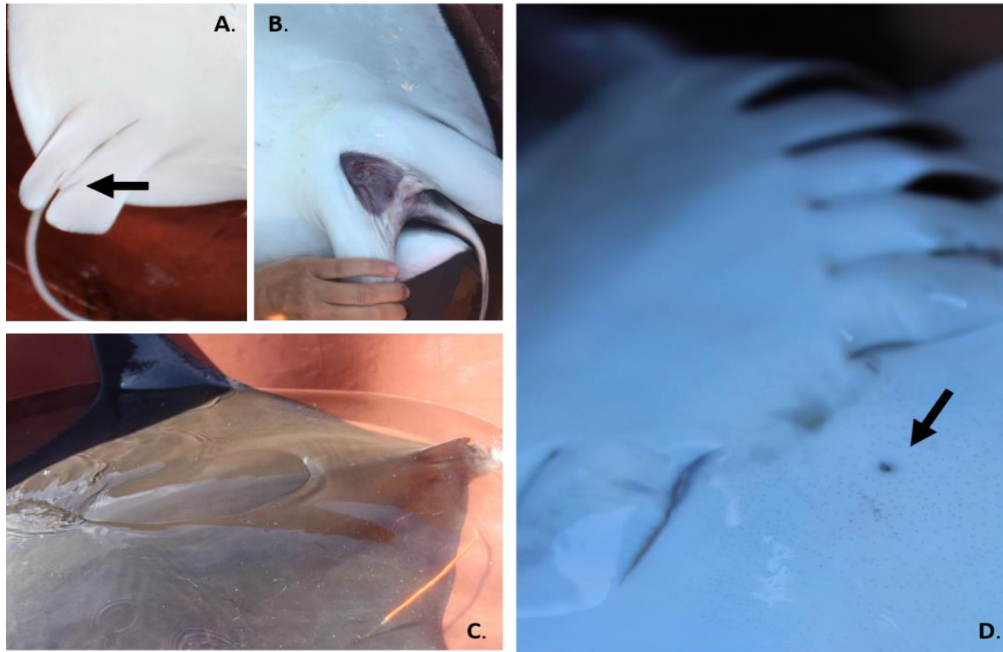


Figure 4. **A)** Juvenile male Munk's devil ray with undeveloped claspers (pointed with an arrow) collected at EG during August 2017. **B)** Adult female Munk's devil ray with a distended cloaca collected during April 2018. **C)** A pregnant female with a traditional tag at EG collected in June 2018. **D)** Neonate with the scar of the umbilical cord (indicated by an arrow) in August 2017.

Seven recaptures (6.23%) of 6 individuals were recorded during the period of study. Details of the Munk's devil ray sex, disc width, maturity stage, position and date of capture and recapture are given in **Table 1**. All recaptured devil rays had equal or smaller straight line capture/recapture distance of 0.5 km from their capture location, with recapture durations ranging from 1 day to 8 months from initial capture.

At the time of tagging disc width distribution of recaptured devil rays was not statistically different from disc width distribution of all captured devil rays ($X^2 = 48.165$, $df = 41$, $p = 0.2055$). This suggests recapture was not affected by size at tagging. No correlation was found between disk width at recapture and distance travelled ($r = -0.236$, $p = 0.609$). Travelled distance also remained statistically unrelated by sex ($t = 2.3686$, $df = 1.0705$, $p = 0.2409$) and maturity stage ($t = -1.417$, $df = 1.1173$, $p = 0.3729$) among neonates and juveniles.

Table 1. Release and recapture details for tagged Munk’s devil rays. **Ind** is the number of the tag of the individual. **DW** (cm) is the disc width of the individual. **GR** (cm) is the growth rate, difference between DW at recapture and DW at tagging. **DL** are the days at liberty of the individual from the day it was tagged until its recapture. **TD** (Km) is the travelled distance.

Ind	Capture						Recapture							
	Latitude	Longitude	Date	Sex	DW (cm)	Maturity Stage	Latitude	Longitude	Date	DW (cm)	GR (cm)	Maturity Stage	DL	TD (Km)
346	24.56103°	-110.395300°	02/08/2017	M	70.5	Juvenile	24.56192°	-110.394680°	07/10/2017	74	3.5	Juvenile	66	0.12
363	24.56103°	-110.395300°	02/08/2017	M	75	Juvenile	24.56192°	-110.394680°	07/10/2017	78.5	3.5	Juvenile	66	0.12
441	24.56159°	-110.395310°	03/08/2017	M	55	Neonate	24.55973°	-110.396270°	08/10/2017	60	5	Juvenile	66	0.22
441	24.55973°	-110.396270°	08/10/2017	M	60	Juvenile	24.56066°	-110.395600°	03/12/2017	64	4	Juvenile	56	0.12
361	24.56192°	-110.394680°	07/10/2017	F	51	Juvenile	24.55973°	-110.396270°	08/10/2017	51	0	Juvenile	1	0.29
392	24.55973°	-110.396270°	08/10/2017	M	49	Juvenile	24.56066°	-110.395600°	03/12/2017	52.5	3.5	Juvenile	56	0.13
351	24.56159°	-110.395310°	03/08/2017	F	50	Neonate	24.55757°	-110.397257°	06/04/2018	65	15	Juvenile	246	0.5

Acoustic Telemetry

Seven Munk’s devil rays were passively tracked during 2017/2018, four neonates (50-55 cm DW) and three juveniles (72-75 cm DW). The seven tags were recorded by at least two receivers around the ESA. Acoustic deployments durations were inferred to range from 80–315 days according to dates of first and last detection on the array (236 ± 89 , mean \pm SD). We recorded 36,836 detections for all individuals at 4 of the 6 receivers placed around ESA during the monitoring period (8/2017–6/2018) (**Table 2**).

Residency

Overall residency index ranged from 0.03 to 0.58 (0.29 ± 0.22 , mean \pm SD) at the ESA. The time on which detections were received for the individual Munk’s devil rays ranged from 9 to 167 d (85.7 ± 65.04 d, mean \pm SD). Detections on consecutive days were found in receivers within EG (RS1 and RS2; maximum 145 consecutive days) and outside EG (RS3; maximum of 3 consecutive days). Neonate individuals were present at EG during 26 to 145 successive days while juveniles ranged from 1 to 17 days.

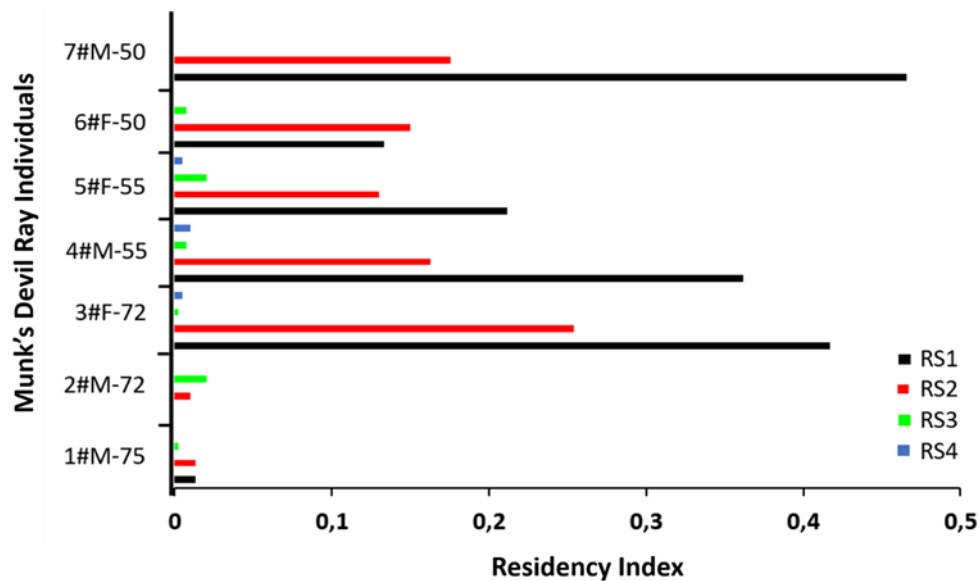


Figure 5. Residency index (RI) of Munk’s devil rays tagged at EG with internal acoustic transmitters. RI is given for each receiver station (RS) located around the ESA. Individual devil rays (Number #Sex- Disc width in cm) are arranged by increasing disk width from top to bottom.

Habitat preference

Areas of high activity as determined by number of detections of tagged Munk’s devil rays were in coastal waters inside EG receivers (RS1, RS2). These two receivers yielded 98.7% of the validated detections, while the offshore receiver never detected tagged rays (RS5). The receivers placed at EG (RS1, RS2) revealed a statistically higher index of residence than the rest of the receivers placed around the ESA ($W_{26} = 182$, $p = 0.0001$) (**Fig. 5**).

Table 2. Passive acoustic details for tagged Munk’s devil ray. **TDATE** is the tagging date. **Loc** is the tagging location. **N Days** is the total number of days with a detection anywhere within the array. **MCD** is the maximum number of consecutive days the individual was detected at EG. **DUR** is the duration between date of tagging and the last day detected. **N Hits** is the total number of detections for each individual. **MLD** is the minimum linear dispersal distance between two furthest receivers with detections (Km). **RI ESA** is the residency index for the entire array around ESA.

Individual	Sex	DW (cm)	Maturity Stage	T Date	Location	N Days	MCD	DUR	N hits	MLD	RI ESA
1	F	75	Juvenile	02/08/2017	EG	9	3	211	27	21.44	0.03
2	F	72	Juvenile	01/08/2017	EG	11	1	294	181	21.55	0.04
3	M	72	Juvenile	01/08/2017	EG	167	17	302	3214	21.44	0.54
4	F	55	Neonate	02/08/2017	EG	130	70	293	8972	21.44	0.42
5	M	52	Neonate	02/08/2017	EG	82	26	315	4231	21.5	0.27
6	M	50	Neonate	02/08/2017	EG	51	46	80	4778	21.44	0.17
7	F	50	Neonate	02/08/2017	EG	150	145	159	15433	1.22	0.58

Seasonality

Acoustic detections occurred at EG throughout the year for most devil rays, with statistically significant differences in their residency index throughout months (Kruskal-Wallis $X^2= 18.394$, $df = 10$, $p=0.04868$). The significant differences were found comparing: (1) August 2017 vs April 2018, (2) June 2018 vs August and December 2017, (3) May 2017 vs August 2017, (4) October 2017 vs April 2018, (5) September 2017 vs January, April and June 2018 (Dunn test for all comparisons, $p<0.05$) (**Fig. 9**). The highest residency index was found during August, September and December of 2017. From the middle of April 2018, neonates were no longer detected inside EG coinciding with the appearance of adults in the outer part of EG.

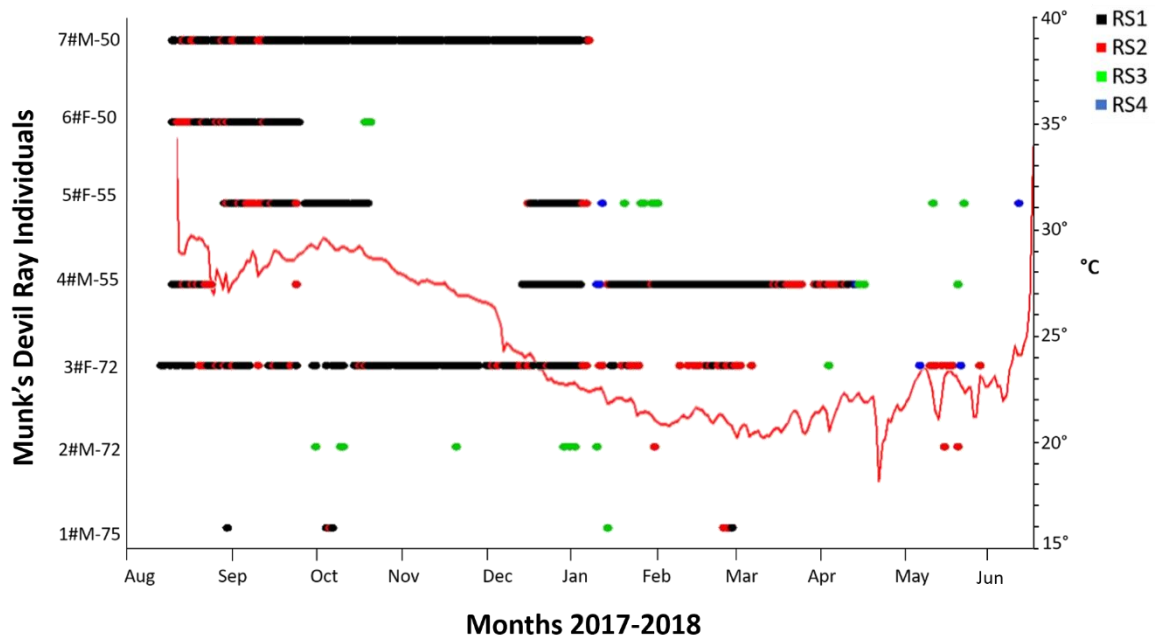


Figure 6. Timeline showing the days each individual Munk’s devil ray was detected in the ESA, from August 2017 to June 2018 with the specific location of each detection color coded. Solid red line indicates mean daily water temperature at EG. Individual devil rays (Number #Sex- Disc width in cm) are arranged by increasing body size from top to bottom.

Movements

A minimum linear dispersal distance (MLD) of 21.5 and 21.4 km was estimated based on detections around the ESA for 6 of the 7 individuals acoustically tagged. One neonate individual was never detected outside of EG, and had an MLD of only 1.22 km. The neonate individual #4 traveled an MLD of 21.4 km during a two-days period. This individual was detected in EG (RS1) at noon and again 12 h later at RS4, 9.3 km away. After one day at RS4 the individual was detected at RS3, 12.2 km away.

Diel change

All detections at EG (RS1 and RS2) showed that the spatial distribution of Munk’s devil rays varied by time of the day (**Fig. 7**). Tagged Munk’s devil rays were detected mostly by coastal receiver (RS1, 5 m depth) during all hours of the day

and night but did not follow a uniform frequency detected rate ($U=359.6$, $p<0.05$), being significantly more frequent during daytime and from 02:00 am to 05:00 h. We found two peaks in detections between 7 am to 16 pm, and 2 am to 5 am. In contrast, the receiver placed further offshore in EG (RS2, 26 m depth) showed a significant diel difference in detection rate ($U=359.39$, $p<0.05$) with detections recorded mostly during daytime and almost no detections during nighttime when *M. munkiana* seem to move to shallower areas (RS1).

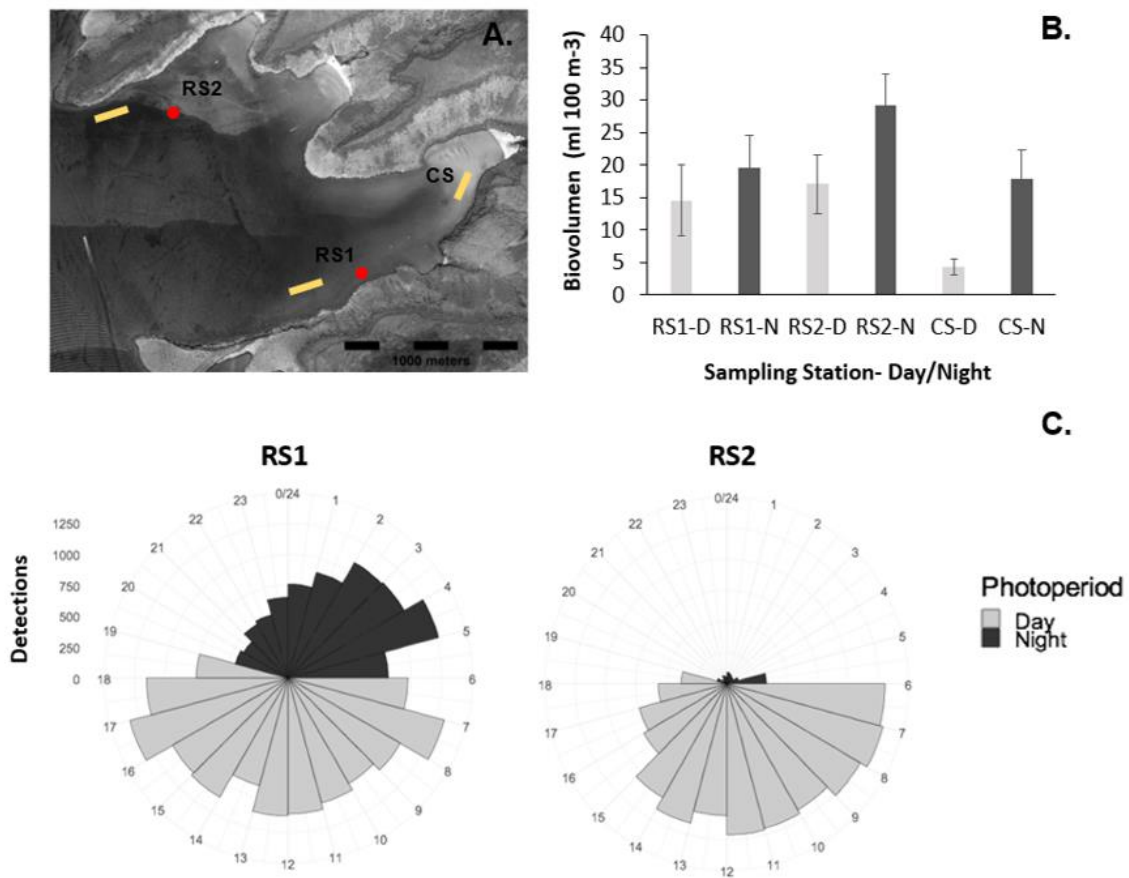


Figure 7. A) Satellite image of EG. Red dots indicated receiver stations, RS1 shallow receiver (5 m depth) and RS2 deeper receiver (26 m depth). Yellow lines represent the zooplankton sampling stations, RS1, RS2 and coastal station (CS). **B)** Mean zooplankton biovolume per sampling station at EG during day and night time. Standard error are represented in black lines. **C)** Circular plots showing hours of detections for all Munk’s devil rays (n= 7) at the two receivers of EG. A significant non-uniform distribution of the detections was registered for both receivers ($p<0.05$).

Environmental Factors

Temperature

Sea water temperature from EG was recorded from August 19, 2017 until the recovery of the acoustic receivers June 6, 2018. Temperature values followed the seasonal pattern (Obeso-Nieblas *et al.*, 2002) with maximum temperatures from June to November (22.2–33.3°C) and minimum values from December to May (16.0–26.5°C). About 77% of hits recorded in EG occurred from 25.5–30.2 °C within a range of 16.0 to 33.3°C. We found a statistically significant Spearman correlation between the water temperature and the mean monthly residency index of tagged Munk's devil rays at EG ($S = 2.496e+09$, $p < 2.2e-16$, $\rho=0.643$) (**Fig. 8**). During August when neonates were captured at EG the temperature ranged from 25.8– 30.2°C. The four neonate individuals were detected at EG when the temperature ranged from 18.8–29.6°C. The adults were captured at sea water temperature ranging from 16.0°C to 29.1°C.

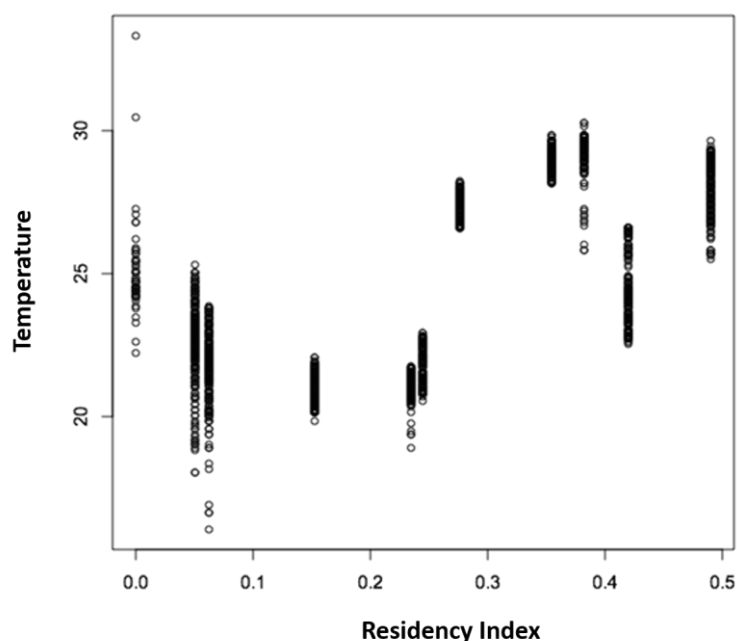


Figure 8. Relationship between the mean monthly residency index (RI) and the daily sea water temperature recorded at EG during each month ($S = 2.496e^9$, $p < 2.2e^{-16}$, $\rho=0.643$). Higher water temperatures resulted in higher residency index for juveniles and neonates Munk's devil ray.

Zooplankton

Zooplankton was mostly composed by major taxonomic groups of holoplankton (Copepoda, Cladocera, Euphausiida, Chaetognatha, Mysidacea and Decapoda). On a preliminary analysis of the zooplankton composition on the samples collected, we observed that *N. simplex* was caught at RS1 in higher abundance and more often than in CS and RS2. On the other hand, Mysidacea spp were more frequently found in the shallower part, the costal station of EG.

Zooplankton biovolume was significantly greater during the night compared to day ($W_{126} = 1175$, $p = 0.0001549$) across all sampling months, with a peak value of 36.27 ± 8.25 mL 100 m^{-3} (mean \pm SE) during nighttime samples in December and minimum during the daytime in October (7.77 ± 9.24 mL 100 m^{-3} , mean \pm SE). We found a significantly higher mean zooplankton biovolume during the cold season (December to May) ($W_{125} = 2454.5$, $p = 0.027$) with significant differences among months (Kruskal-Wallis $X^2 = 23.1$, $df = 5$, $p = 0.0003$), (1) April 2017 vs. December 2017, (2) August 2017 vs. June 2018, (3) October 2017 vs. August and December 2017 (Dunn test for all comparisons, $p < 0.05$). Maximum zooplankton biovolume values were observed during December 31.12 ± 4.98 mL 100 m^{-3} (mean \pm SE) and the lowest values in June 10.91 ± 1.64 mL 100 m^{-3} (mean \pm SE) (**Fig. 9**).

We found significant differences of zooplankton biovolume among our three sampling stations inside EG (Kruskal-Wallis $X^2 = 13.478$, $df = 2$, $p = 0.00118$) between the RS2 station vs the RS1 and the coastal station (Dunn test, $p < 0.05$). RS2 was the station with a higher mean zooplankton biovolume recorded at night time, 29.13 ± 4.89 mL 100 m^{-3} (mean \pm SE). However, Munk's devil rays were mainly detected during night hours at the RS1 where zooplankton biovolume mean value was low 19.55 ± 5.08 mL 100 m^{-3} (mean \pm SE).

Mean monthly residency index at EG and the zooplankton biovolumen within EG were significantly positively correlated ($S = 221340$, $p = 5.046e-05$, $\rho = 0.3516104$).

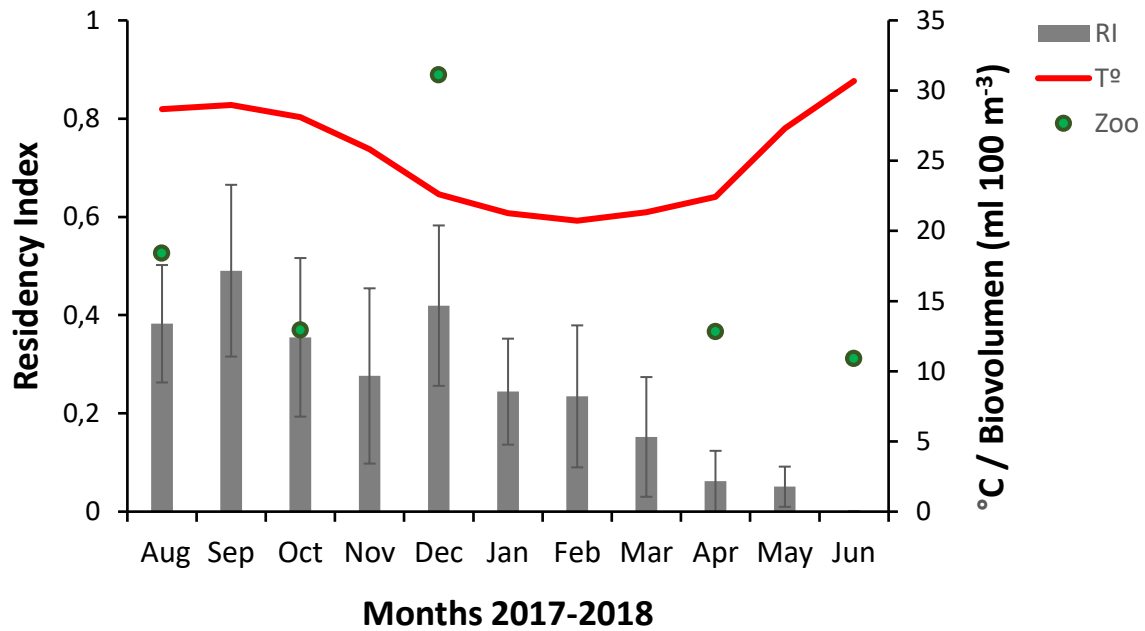


Figure 9. Mean monthly residency index at EG for all Munk’s devil rays ($n=7$). The vertical lines represent the standard error (SE) for each month’s residency index. Red line is the mean monthly temperature at EG and green dots are the mean monthly zooplankton biovolume.

Stable Isotopes Analysis

Devil rays

We obtained the isotopic values for $\delta^{13}\text{C}$ and $\delta^{15}\text{N}$ from 69 *M. munkiana* blood samples at ESA. During the warm season of 2017 blood was collected from 9 adults, 18 juveniles, 9 neonates and during the cold season 2018, 5 adults, 2 pregnant adults and 26 juveniles (**Table 3**). Stable isotopes values for *M. munkiana* ranged from -18.45‰ to -15.27‰ for $\delta^{13}\text{C}$ and from 14.55‰ to 17.51‰ for $\delta^{15}\text{N}$. We found no significant differences in isotopic values between ray sexes or between cold and warm seasons (Wilcoxon test, $p > 0.05$). However, we found significant differences in the isotopic values for $\delta^{13}\text{C}$ (Kruskal-Wallis $X^2 = 27.08$, $df = 3$, $p = 5.641e^{-6}$) and $\delta^{15}\text{N}$ among maturity stages (Kruskal-Wallis $X^2 = 7.97$, $df = 3$, $p = 0.04$). The mean $\delta^{13}\text{C}$ of juveniles is significantly enriched than adults and pregnant females; neonates also had enriched $\delta^{13}\text{C}$ values than adults. The $\delta^{15}\text{N}$ showed significant differences between neonates vs juveniles and adults with enriched $\delta^{15}\text{N}$ values (Dunn test, $p < 0.05$).

Table 3. Stable isotopes summary information for blood tissue collected from *M. munkiana* during 2017-2018 at ESA. All values are means \pm SD.

Maturity Stage	Season	N ^o of samples	DW (cm)	Tissue turnover (mean, d)	$\delta^{15}\text{N}$ (‰)	$\delta^{13}\text{C}$ (‰)	Bulk C:N	Trophic Position
Neonates	Warm	9	52.02 \pm 1.91	87	16.96 \pm 0.49	-16.83 \pm 0.26	2.35 \pm 0.09	3.33 \pm 0.21
Juveniles	Warm	18	72.47 \pm 8.70	87	16.19 \pm 0.62	-16.51 \pm 0.27	2.41 \pm 0.10	2.99 \pm 0.27
Juveniles	Cold	26	78.69 \pm 10.81	87	16.51 \pm 0.50	-16.69 \pm 0.55	2.27 \pm 0.09	3.13 \pm 0.21
Adult	Warm	9	101 \pm 3.12	87	16.28 \pm 0.46	-17.45 \pm 0.644	2.46 \pm 0.05	3.03 \pm 0.20
Adult	Cold	5	106.9 \pm 4.33	87	16.6 \pm 0.18	-17.9 \pm 0.14	2.3 \pm 0.13	3.15 \pm 0.08
Pregnant female	Cold	2	109.5 \pm 2.12	87	16.4 \pm 0.01	-17.8 \pm 0.07	2.4 \pm 0.02	3.10 \pm 0.005

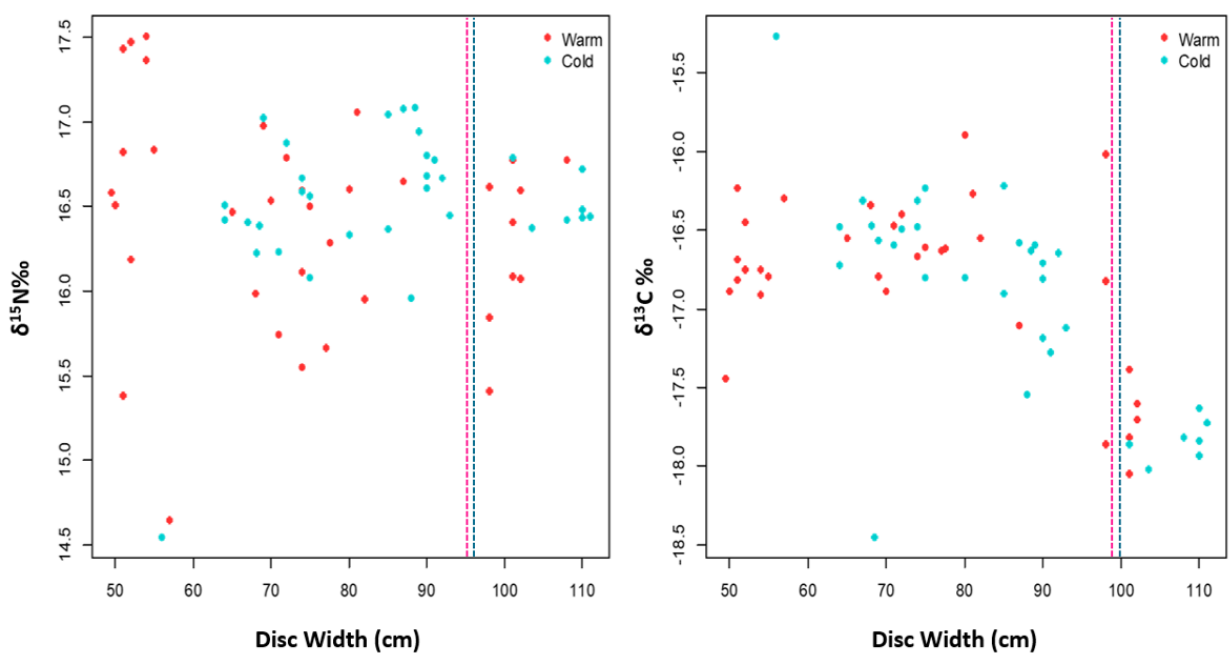


Figure 10. $\delta^{15}\text{N}$ and $\delta^{13}\text{C}$ values for *M. munkiana* during cold (blue) and warm (red) season at ESA during 2017-2018. Points represent the $\delta^{13}\text{C}$ and $\delta^{15}\text{N}$ blood values from each individual. Disc width at which females (97 cm) and males (98 cm) attain adulthood is shown with dotted pink and blue lines, respectively.

Isotopic niche breadth and trophic overlap

Stable Isotope Bayesian Ellipses (SIBER) were used to determine niche breadth and trophic overlap among the different Munks' devil ray maturity stages. Considering the standard corrected ellipse area SEAc, juveniles (0.82) have a greater niche breadth than neonates (0.42) or adults (0.43). It was not possible to calculate pregnant females SEAc because of the low sample number (n=2).

The niche overlap among juveniles (20.9%) and neonates (40.4%) was higher for the last one due to its smaller niche breadth (**Fig. 11B**).

Trophic position

Trophic position of each maturity stage of *M. munkiana* was calculated using Post (2002) equation during the warm and cold seasons. The mean $\delta^{15}\text{N}$ value of 13.90 ‰ baseline was estimated from the zooplankton samples collected during the cold season at EG. Using this, we estimated an overall trophic position of 3.11 ± 0.24 (mean \pm SD) for *M. munkiana* at ESA. Trophic position did not vary across seasons (Wilcoxon test, $p > 0.05$) but neonates occupied a higher trophic position compared to the other age classes (3.33 ± 0.21 , mean \pm SD) (Kruskal-Wallis $X^2 = 7.97$, $df = 3$, $p = 0.0465$) (**Table 3**), likely due to trophic enrichment from the mother.

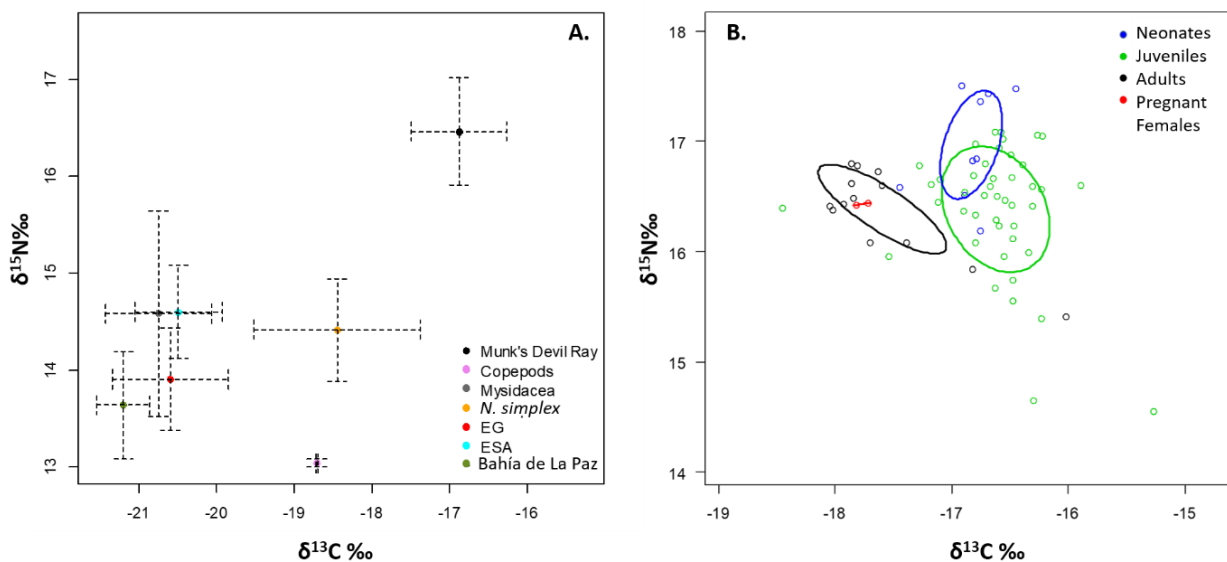


Figure 11. A) Isotopic values for $\delta^{13}\text{C}$ and $\delta^{15}\text{N}$ from Munk's devil ray blood, preys and zooplankton collected during the cold season at the EG, ESA and Bahía de La Paz. Points are mean values and dotted lines are the standard deviation for each group. **B)** Isotopic niche overlapped among *M. munkiana* maturity stages. Points represent the $\delta^{13}\text{C}$ and $\delta^{15}\text{N}$ blood values from each individual. Standard ellipses were calculated using Bayesian statistics with the SIBER analysis.

Zooplankton

Twenty zooplankton samples were collected during the cold season 2017–2018. The samples of *M. munkiana*'s prey taxonomic groups, $\delta^{13}\text{C}$ values ranged from -18.45 ‰ (Euphausiids, *N. simplex*) to -20.75 ‰ (Mysidacea) and $\delta^{15}\text{N}$ values differed among taxonomic groups (ANOVA, $p < 0.01$). The $\delta^{15}\text{N}$ values ranged from 13.04 ‰ (Copepods) to 14.58 ‰ (Mysidacea) and they were not significantly different (ANOVA, $p > 0.05$). There were no significant differences $\delta^{15}\text{N}$ and $\delta^{13}\text{C}$ values among sampling stations (EG, ESA and Bahía de La Paz) (Kruskal-Wallis test, $p > 0.05$) (**Table 4**).

Trophic fraction

All the taxonomic zooplankton groups and all the sampling stations were depleted in $\delta^{15}\text{N}$ and $\delta^{13}\text{C}$ in comparison to Munk's devil rays (**Table 4**). Trophic fractionating was calculated for each devil ray individual with the mean value for each zooplankton taxonomic group. The $\delta^{15}\text{N}$ fractionating of the prey taxonomic groups ranged from 1.94 ‰ (Mysidacea) to 3.48 ‰ (Copepods) and $\delta^{13}\text{C}$ from 1.51 ‰ (Euphausiids, *N. simplex*) to 3.81 ‰ (Mysidacea).

The variability of $\delta^{13}\text{C}$ was smaller among areas with values ranging from 1.92 ‰ (ESA) to 2.88 ‰ (Bahía de La Paz) and in $\delta^{15}\text{N}$ values ranged from 3.55 ‰ (ESA) to 4.26 ‰ (Bahía de La Paz).

Table 4. Stable isotopes summary for zooplankton samples collected during the cold season 2017-2018. All values are means \pm SD. *Mean trophic fractionation between Munk's devil rays and the mean value for each zooplankton taxonomic group.

Zooplankton Group	Season	Nº of samples	$\delta^{15}\text{N}$ (‰)	$\delta^{13}\text{C}$ (‰)	Bulk C:N	$\Delta \delta^{15}\text{N}$ (‰)*	$\Delta \delta^{13}\text{C}$ (‰)*
<i>N. simplex</i>	Cold	3	14.42 \pm 0.52	-18.45 \pm 1.07	4.91 \pm 0.71	2.10	1.51
Copepods	Cold	2	13.04 \pm 0.04	-18.71 \pm 0.01	4.47 \pm 0.02	3.48	1.77
Mysidacea	Cold	3	14.58 \pm 1.06	-20.75 \pm 0.68	4.62 \pm 0.36	1.94	3.81
All groups EG	Cold	4	13.90 \pm 0.52	-20.60 \pm 0.74	5.65 \pm 0.65	2.62	3.66
All groups ESA	Cold	5	14.60 \pm 0.48	-20.49 \pm 0.56	5.73 \pm 0.63	1.92	3.55
All groups La Paz Bay	Cold	3	13.64 \pm 0.55	-21.20 \pm 0.34	6.49 \pm 0.78	2.88	4.26

DISCUSSION

Nursery Area

Using the criteria proposed by Heupel *et al.* (2007) and Martins *et al.* (2018), The Ensenada Grande bay of the Espiritu Santo Archipelago can be considered a nursery area for *M. munkiana*.

The first criterion that rays are more commonly encountered in EG than in other areas is met by the high relative abundance 86% (n=80) of neonates and juveniles with disk width range of 49-85 cm compared with other studies in the Southern Gulf of California. Notarbartolo di Sciara (1988) and Lopez (2009) captured *M. munkiana* in other near ESA localities in similar disk width range but lower proportions for neonates (8.3 %, n=2) and juveniles (15 %, n= 22) as observed in the present study.

EG fulfills the second nursery area criterion as neonates and juveniles exhibited high residency index to this inshore area having higher proportion of records in coastal acoustic receivers than offshore acoustic receivers placed around the ESA and Bahía de La Paz. Munk's devil rays were detected almost daily for up to 7 of the 11 months monitoring period in the bay. Individuals resided inside EG from 1 to 145 consecutive days. Moreover, recaptured data from traditional tagging demonstrated a site fidelity of two to eight months inside EG for neonates and juveniles.

There is evidence that *M. munkiana* neonates and juveniles inhabit EG repeatedly during several years observing reports of individuals within these early stages since 2013 to 2018 (**Fig. 12**) according with the third criteria to define a nursery area. This information was obtained from recreational divers and ecotourism agencies operating at the ESA. Since ecotourism activities started in 2013, sightings were common each year from September to December. Recreational divers used to observe feeding aggregations of neonate and juvenil individuals during night dives at shallow areas of EG (< 6 m). These observations constitute an example of the potential value about how historical observations done by recreational divers at aggregations sites provide new insights into seasonality and species distribution (Luiz *et al.*, 2008; Stewart *et al.*, 2018b).

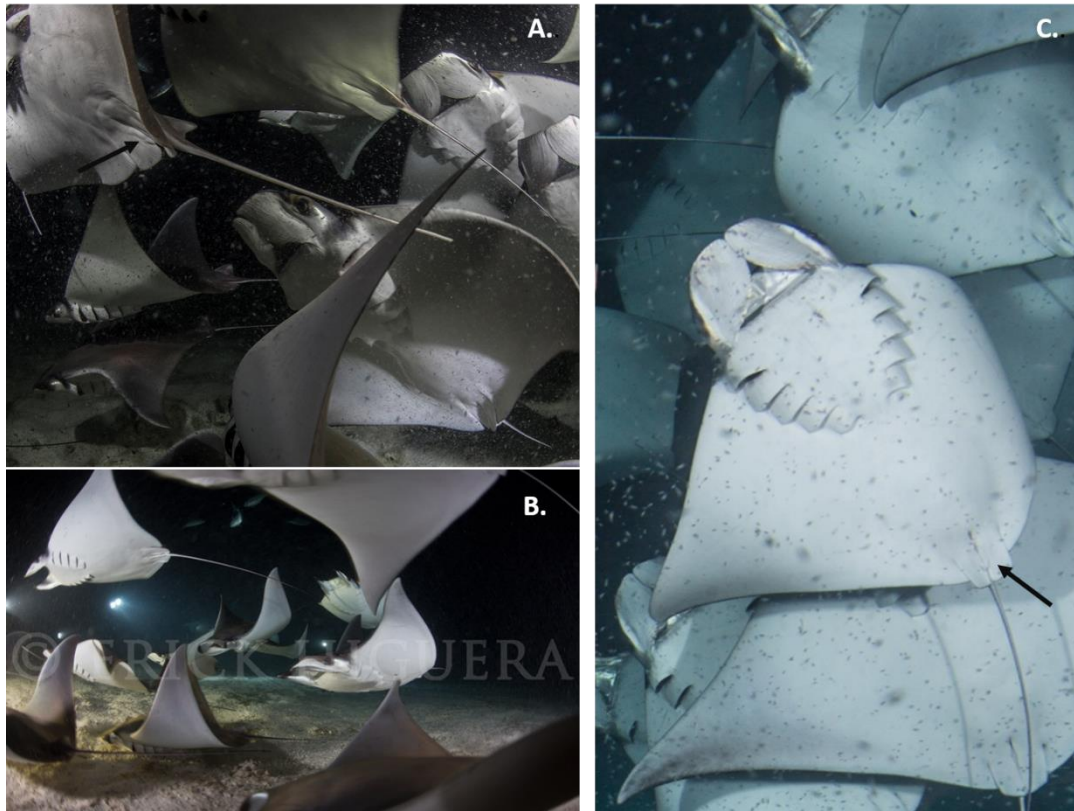


Figure 12. Juvenile Munk's devil ray feeding at night in EG during recreational night dives. **A)** November 2013; **B)** October 2014; **C)** October 2016. Undeveloped claspers are indicated with arrows. Photograph copyrights: **A** and **B.** Erick Higera; **C.** Luke Inman.

Collectively, these observations provide compelling evidence that *M. munkiana* uses EG as a nursery area during their early life stages. Furthermore, according to Bass (1978) this area can be described as a primary nursery area due to the presence of neonates and near-term pregnant females, and as a secondary nursery area because of the presence of juveniles (non-newborn). Therefore, overlapping of primary and secondary nursery areas for *M. munkiana* at EG occurs, similar as observed for other elasmobranch species (Snelson *et al.*, 1984; Heupel *et al.*, 2007).

Segregation by Size and Sex and Mating Season

We observed a clear ontogenetic spatio-temporal segregation in the distribution of Munk's devil ray at EG during our tagging trips. Neonates, juveniles, and adults were all caught in different time of the day and areas in EG. Neonates and

juveniles were mostly distributed at shallower areas (2-10 m depth) while adults were observed at the deeper areas (>15 m depth) of EG. Size segregation appears to be a common feature for this and other species of mobulids (Notarbartolo-di-Sciara, 1988; Deakos, 2010).

Although sex segregation has been reported in the southern part of the Gulf of California across different years for mainly adults individuals of *M. munkiana* (Notarbartolo Di Sciara, 1988; Villavicencio-Garayzar, 1991; Guerrero-Maldonado, 2002; Lopez, 2009), we found a 1:1 sex ratio for neonates and juveniles, a typical feature on elasmobranch nursery areas (Castro, 1993; Salomon *et al.*, 2009; Trejo, 2017). This suggests that *M. munkiana* does not segregate by sex during early stages until they reach sexual maturity when sex segregation may occur.

Size at maturity is reported for 97-98 cm disk width for female and male respectively (Lopez, 2009), however we proposed that individuals from 85 cm disk width up to maturity size are subadults (sexually immature) with a higher mobility and therefore, a lower degree of site fidelity. 13 Subadults (85–93 cm DW) were caught during April 2018 in other bays of ESA in schools where adults were also present. All male individuals (n=8) had undeveloped claspers with little calcification and without semen. We did not catch any subadult individual at the shallow part of EG (<10 m depth).

Munk's devil ray is the only mobulid species in the Gulf of California that is consistently seen in dense schools (Notarbartolo-di-Sciara,1988). They progressively increase in numbers of individuals within schools as individuals increased their body size from neonates to adults. At ESA small schools of neonate individuals (< 7 individuals) are observed at shallow areas while dense schools of adults (>100) appear during the pupping season at deeper areas.

Aggregations of adults displaying courtship behavior at the surface, were observed at depths > 15 m at EG during April and June. It is very likely that mating behavior occurs soon after giving birth for *M. munkiana* since courtship and pregnancy were observed in the same area and period. Our field observations are supported by the mating behavior after parturition observed in captivity (Uchida *et al.*, 2008) and wild individuals of *M. alfredi* (Stevens *et al.*, 2018).

Females with swollen and distended cloaca were captured in April 2018. A distended cloaca has been interpreted as evidence of a recent mating feature in other elasmobranch species (Carrier & Jeffrey, 2012).

Pupping Season

Reproductive seasonality has been documented for several mobulid species (Marshall & Bennett, 2010; Stevens, 2016; Stevens *et al.*, 2018). Based on our captures and field observations we hypothesized that the pupping season for Munk's devil rays begin in April and ends in June with temperatures between 16–29°C. Neonates (mobulas with umbilical cord scars) and juveniles were captured in the shallow area of EG. However, neonates were found only during August 2017 while juveniles were caught during all sampling months. Parturition for Bahía de La Paz also has been previously reported elsewhere between May and June (Villavicencio-Garayzar, 1991), corroborating our observations.

This time frame coincides with the end of the cold season and the cold-warm transition (June) when the euphausiid, *Nyctiphanes simplex*, one of the two main *M. munkiana* preys (Hobro, 2002) attain its maximum abundance and reproductive period in the Gulf of California (Brinton & Townsend 1980; De Silva Dávila & Palomares-García, 1998; Gómez-Gutiérrez *et al.*, 2012). The lowest abundance of *N. simplex* occurs between July and October (Brinton & Townsend, 1980) when adult *M. munkiana* have not been observed in the ESA. We did not find a positive correlation between zooplankton biovolume and presence of *M. munkiana* adults. However, we suggest that large mating aggregations of Munk's devil ray around the ESA benefit from the secondary production rates reported in Bahía de La Paz during the pupping season, with peaks of up to 44.2 mL 100 m⁻³ for these months (De Silva Dávila & Palomares-García, 1998).

Near-term pregnant females were caught during April 2018 at the ESA and early June 2018 at EG. The pregnancy of a near-term female captured at the ESA during our tagging trips was corroborated using ultrasound techniques, with a single and well-developed term-embryo (Ramírez *et al.*, 2018 in prep). This corroborated the estimation of the gestation of a single pup for *M. munkiana* (Villavicencio-Garayzar, 1991) and other mobulis species (Marshall *et al.*, 2009; Couturier *et al.*, 2012).

Mobulids present an embryonic nutrition where embryos develop and receive nutrition from its mother's uterus, feeding initially on the yolk, which leaves the umbilical cord scar. This scar can be closed already during the last embryo stages (Galvan-Magaña, pers. obs). Thus, the embryo nourished with protein and lipid-rich histotroph, secreted by the mother's uterine villi (Wourms, 1977; Dulvy & Reynolds, 1997; Compagno & Last, 1999). This establishes an energy connection where nutrients are transferred directly from the mother to the embryo resulting in an isotopic enrichment of $\delta^{15}\text{N}$ values and similar or depleted $\delta^{13}\text{C}$ values in the neonates in comparison to the mother (Porrás-Peters *et al.*, 2008; Elorriaga-Verplancken *et al.*, 2013).

In the present study we found neonates with umbilical cord scars had significant enrichment in $\delta^{15}\text{N}$ values of up to 2.10‰ compared to adults. This $\delta^{15}\text{N}$ mother transferred enrichment is similar to the consumer-prey enrichment values reported for elasmobranchs evidenced with blood serum 2.2 ± 0.7 ‰ and 2.4 ± 0.5 ‰ red blood cells (mean \pm SD) (Kim *et al.*, 2012). Using Caut *et al.* (2013) information, a turnover rate of blood tissue of 87 days for elasmobranch was calculated (Trejo, 2017). Therefore, neonate individuals with enriched $\delta^{15}\text{N}$ values captured in August should have been in their mother uterus approximately during May, which coincides within our proposed reproductive and pupping season.

Habitat Use of Neonates and Juveniles

The Southern Gulf of California was previously thought to be a wintering ground for *M. munkiana*, which after that migrated into unknown areas during warmer seasons for mating and pupping (Notarbartolo-di-Sciara, 1988). However, Villavicencio-Garayzar (1991) observed mating behavior during spring at Bahía de La Paz. We propose the use of a shallow bay, EG as a nursery area where neonate and juvenile females and males in same sex proportion remain in the area throughout the year. Neonates and juveniles were detected frequently at EG during late summer, autumn (warm season), winter and the beginning of the spring (cold season).

Tagged individuals showed a higher consistency on their detections from August to April when water temperature ranged from 18.8–29.6°C, with up to 145 d consecutive detections suggesting that they may range less widely at those

months of the year. Munk's devil ray during their early life stages exhibited a higher residency index at warmer water temperatures. This residency may provide an ecological advantage for the species accelerating metabolic rates (feeding and growth) of juveniles and thus reducing the duration of these vulnerable life-history stages (Tenzing, 2014; Wearmouth & Sims, 2008; Heuple *et al.*, 2007).

Detection rates for all tagged individuals decreased during March and April when adults began to be frequent at EG and ESA. For larger juveniles observed in April and June, this period represents the recruitment time based on field observation of a traditional tagged juvenile (about 85 cm disk width) swimming on the deep part of EG (>20 m) adding to large schools of Munk's devil ray adults.

The greatest number of detections (independently of the day-night time) were at RS1 receiver at 5 m depth placed at the southern entrance of EG (**Fig. 10**). The location of the RS1 was not the area where the highest zooplankton biovolume was observed at EG; however, during zooplankton tows carried out at this station, *N. simplex* was caught in high abundance and more often than in the other two sampling stations inside EG. This is an interesting observation since this species seem to attain their highest population densities at 50–100 m depth regions in the Gulf of California (Gómez-Gutiérrez *et al.*, 2012).

The high abundance of *N. simplex* at near coastal waters can partially explain the higher detection rate of *M. munkiana* recorded at RS1. On the shallower and inner part of EG (CS station) Mysidacea spp. were more frequently found at bottom depth (>5 m). During the capture trips, neonates and juveniles were only found in these two portions of the bay within depths < 10 m.

The differential habitat preference between neonates, juveniles, and adults was also evidenced using stable isotopes of blood tissue. $\delta^{13}\text{C}$ values showed significant differences between ontogenetic stages, similar as the results obtained at other locations in the southern Gulf of California for *M. munkiana* (Cerutti, 2005). Adults had depleted $\delta^{13}\text{C}$ values than neonates and juveniles indicating feeding preferences on more pelagic habitats (France, 1995). Neonates and juveniles showed ^{13}C enrichment relative to ^{12}C explained by their coastal habitat due the influence of terrestrial detritus (France, 1995). Although isotopic niche is not the necessarily the same that trophic niche, they are highly

correlated and provides ecologically relevant information about the individual, population or community studied (Jackson *et al.*, 2011). Isotopic niche overlap among juveniles and adults or neonates and adults was not evidenced using SIBER standard ellipses. The filter-feeders mechanism to enable trophic niche partitioning among different body sizes is less evident than in other elasmobranches (Stewart *et al.*, 2017). For *M. munkiana*, neonates and juveniles behave as residents with a high fidelity to shallow-coastal habitats while adults are more mobile and pelagic organisms. Adult Munk's devil ray individuals were tagged at the north part of Bahía de La Paz showing a more mobile behavior, being detected two weeks later 72 km away from the tagging location (Croll, unpublished observ).

Therefore, the availability of the two main prey, *N. simplex* and mysids for Munk's devil ray and the protection from large predators to early life stages with small sizes and limited swimming ability could favor the use of EG as a nursery area for *M. munkiana*.

CONCLUSIONS

The present study describes for the first time the habitat use and seasonal variability of a nursery area (Heuple *et al.*, 2007) for a *Mobula* species in the Gulf of California. Neonates and juveniles *M. munkiana* individuals were present at ESA during most of the year with a high residency index for a highly mobile and migratory species. Sexual segregation does not occur during early life stages for *M. munkiana* although size segregation is clear. The pupping season goes from April to June. It starts during the cold season associated with the highest zooplankton biovolume values in the region (De Silva-Davila & Palomares-García, 1998).

Residency and site fidelity of neonate and juvenile individuals was positively correlated to warmer water temperatures and higher zooplankton biovolumes. Water temperature was highly correlated to the Munk devil ray's residency index than prey abundance.

Habitat preference among early life stages and adults was also clearly differentiated due to its distribution and its isotopic signals. Adult preferred to

feed on more pelagic habitats while neonates and juveniles were frequently observed at shallow areas of the bays.

Residency index was higher at coastal receivers inside EG and mobulas were present during day and night inside the bay for several months.

EG meets the three previously established criteria to be a primary and secondary nursery area for *M. munkiana*.

This study provides useful biological information for management of the mobula related ecotourism activities at ESA and recognizing critical areas of reproduction to decrease the high rates of bycatch on artisanal fisheries in the region.

REFERENCES

- Alava, E.R.Z., Dolumbalo, E.R., Yaptinchay, A.A. & Trono, R.B. 2002. Fishery and trade of whale sharks and manta rays in the Bohol Sea, Philippines. In: Fowler SL, Reed TM, Dipper FA, editors. Elasmobranch biodiversity, conservation and management: Proceedings of the International Seminar and Workshop, Sabah, Malaysia, July (1997). Cambridge: IUCN Species Survival Commission. 132–148 pp.
- Bass, A.J. 1978. Problems in studies of sharks in the Southern Indian Ocean. *Sensory Biology of Sharks, Skates and Rays. Office of Naval Research, Department of the Navy, Arlington, 545-594.*
- Bizzarro, J.J., Smith, W.D. & Clark, T.B. 2006. *Mobula munkiana*. The IUCN Red List of Threatened Species 2006:e.T60198A12309375 Downloaded on 11 October 2018.
<http://dx.doi.org/10.2305/IUCN.UK.2006.RLTS.T60198A12309375.en>
- Brinton, E. & Townsend, A.W. 1980. Euphausiids in the Gulf of California—the 1957 cruises. *California Cooperative Oceanic Fisheries Investigation Report*, 21:211–236.
- Castro, J.I. 1993. The shark nursery of Bulls Bay, South Carolina, with a review of the shark nurseries of the Southeastern coast of the United States. *Environmental Biology of Fishes*, 38: 37-48.
- Cabana, G. & Rasmussen, J.B. 1996. Comparison of aquatic food chains using nitrogen isotopes. *Proceedings of the National Academy of Sciences (USA)*, 93: 10844–10847.
- Caut S., Jowers M., Lepoint G., Fisk A.T. 2013. Diet and tissue-specific incorporation of isotopes in the shark *Scyliorhinus stellaris*, a North Sea mesopredator. *Marine Ecology Progress Series*, 492: 185-198.

- Cerutti, F. 2005. Isótopos estables de carbono y nitrógeno en mantas (Batoidea: Mobulidae) como indicadores tróficos. Bachelor science dissertation, Universidad Autónoma De Baja California Sur, La Paz, México.
- Cerutti-Pereyra F, Thums M, Austin CM, Bradshaw CJA, Stevens JD, Babcock, RC, Pilland RD, Meekan MG. 2014. Restricted movements of juvenile rays in the lagoon of Ningaloo Reef, Western Australia – evidence for the existence of a nursery. *Environmental Biology of Fishes*, 97(4):371-83.
- Carrier, Jeffrey. 2012. Biology of Sharks and Their Relatives, 2nd Edition.
- Compagno L.J.V., Krupp F., Schneider W. 1995. Tiburones. Guía FAO para la identificación de especies para los fines de pesca. Océano Pacífico Centro-113 Oriental. Food and Agriculture Organization of the United Nations. Roma. 2: 648-743.
- Compagno LJV, Last PR. 1999. Mobulidae: devil rays. In: FAO Species Identification Guide for Fishery Purposes. The Living Marine Resources of the Western Central Pacific. Volume 3. Batoid Fishes, Chimaeras and Bony Fishes, Part 1 (Elopidae to Linophrynidae), Carpenter KE, Niem VH (eds). FAO: Rome, Italy; 1524–1529.
- Couturier, L. I. E., Marshall, A. D., Jaine, F. R. A., Kashiwagi, T., Pierce, S.J., Townsend, K. A., et al. 2012. Biology, ecology and conservation of the Mobulidae. *Journal of Fish Biology*, 80, 1075–1119. doi: 10.1111/j.1095-8649.2012.03264.x
- Croll, D. A., Dewar, H., Dulvy, N. K., Fernando, D., Francis, M. P., Galván-Magaña, F., et al. 2016. Vulnerabilities and fisheries impacts: the uncertain future of manta and devil rays. *Aquatic Conservation Marine and Freshwater Ecosystems*, 26, 562–575. doi: 10.1002/aqc.2591
- Croll, D. A., Newton, K. M., Weng, K., Galván-Magaña, F., O'Sullivan, J., and Dewar, H. 2012. Movement and habitat use by the spine-tail devil ray in the

Eastern Pacific Ocean. *Marine Ecology Progress Series*, 465, 193–200. doi: 10.3354/meps09900

De Silva-Davila R, Palomares-Garcia R. 1998. Unusual larval growth production of *Nyctiphanes simplex* in Bahia de La Paz, Baja California, Mexico. *Journal Crustacean Biology*, 18: 490–498

Deakos, M. H. 2010. Paired-laser photogrammetry as a simple and accurate system for measuring the body size of free-ranging manta rays *Manta alfredi*. *Aquatic Biology*, 10, 1–10. doi: 10.3354/ab00258

Duffy, C. A. J., & Scott, C. T. 2017. First observation of the courtship behaviour of the giant devil ray *Mobula mobular* (Myliobatiformes: Mobulidae). *New Zealand Journal Zoology*, 1–8. doi: 10.1080/03014223.2017.1410850

Dulvy, N. K. & Reynolds, J. D. 1997. Evolutionary transitions among egg-laying, livebearing and maternal inputs in sharks and rays. *Proceedings of the Royal Society B*, 264, 1309–1315.

Dulvy, N. K., Pardo, S. A., Simpfendorfer, C. A., & Carlson, J. K. 2014. Diagnosing the dangerous demography of manta rays using life history theory. *PeerJ*, 2:e400. doi: 10.7717/peerj.400

Elorriaga-Verplancken, F., Auriolles-Gamboa, D., Newsome, S. D., & Martínez-Díaz, S. F. 2012. $\delta^{15}\text{N}$ and $\delta^{13}\text{C}$ values in dental collagen as a proxy for age- and sex-related variation in foraging strategies of California sea lions. *Marine Biology*, 160(3), 641–652. doi:10.1007/s00227-012-2119-y

France R.L. 1995. Differentiation between littoral and pelagic food webs in lakes using carbon isotopes. *Limnology and Oceanography*, 40: 1310–1313.

Gaitan, J; A. Alvarez; C. Martinez, H. Rojas & P. Rojo. 2005. Estudio del medio costero del Complejo Espíritu Santo para su manejo sustentable, Reporte final, p46.

- Gómez-Gutiérrez, J., Martínez-Gómez, S. & Robinson CJ. 2012. Seasonal growth, molt, and egg production of *Nyctiphanes simplex* (Crustacea: Euphausiacea) juveniles and adults in the Gulf of California. *Marine Ecology Progress Series*, 455:173-194. doi: 10.3354/MEPS09631.
- Guerrero Maldonado, L.A. 2002. Captura comercial de elasmobranquios en la costa suroccidental del Golfo de California, México. Bachelor science dissertation, Universidad Autónoma De Baja California Sur, La Paz, México.
- Heinrichs, S., O'Malley, M., Medd, H.B. & Hilton, P. 2011. The Global Threat to *Manta* and *Mobula* Rays. *Manta Ray of Hope*.
- Heupel M., & Simpfendorfer, C. 2002. Estimation of mortality of juvenile blacktip sharks, *Carcharhinus limbatus*, within a nursery area using telemetry data. *Canadian Journal of Fisheries and Aquatic Science*, 59(4): 624–632.
- Heupel, M., Carlson J. & Simpfendorfer, C. 2007. Shark nursery areas: Concepts, definition, characterization and assumptions. *Marine Ecology Progress Series*, 337: 287–297.
- Heupel M., & Simpfendorfer, C. 2011. Estuarine nursery areas provide a low-mortality environment for young bull sharks *Carcharhinus leucas*. *Marine Ecology Progress Series*, 433: 237–244.
- Hidalgo-Gonzalez RM & Alvarez-Borrego, S. 2004. Total and new production in the Gulf of California estimated from ocean color data from the satellite sensor SeaWiFS. *Deep-Sea Research Part II*, 51:739–752
- Hobro, F. 2002. The feeding ecology, foraging behavior and conservation of manta rays (Mobulidae) in Baja California, Mexico. Master science dissertation, University of Wales, Bangor, UK.
- Hoening JM & Gruber SH. 1990. Life-History patterns in the elasmobranchs: implications for fisheries management. In *Elasmobranchs as Living*

Resources: Advances in the Biology, Ecology, Systematics, and the Status of the Fisheries, Pratt Jr HL, Gruber SH, Taniuchi T (eds). US Department of Commerce, NOAA Technical Report NMFS 90: Washington DC; 1–16.

Hussey N.E., Brush J., McCarthy I.D. & Fisk A.T. 2010. $\delta^{15}\text{N}$ and $\delta^{13}\text{C}$ diet–tissue discrimination factors for large sharks under semi-controlled conditions. *Comparative Biochemistry and Physiology Part A: Molecular & Integrative Physiology*, 155(4): 445-453.

Jackson AL, Inger R, Parnell AC & Bearhop S. 2011. Comparing isotopic niche widths among and within communities: SIBER—Stable Isotope Bayesian Ellipses in R. *Journal of Animal Ecology*, 80: 595–602

Lopez, J. N. S. 2009. Estudio Comparativo de la Reproduccion de tres Especies del Genero *Mobula* (Chondrichthyes: Mobulidae) en el Suroeaste del Golfo de California, Mexico. Master science dissertation, Instituto Politecnico Nacional, La Paz, Mexico.

Luiz, O. J., Balboni, A. P., Kodja, G., Andrade, M., & Marum, H. 2008. Seasonal occurrences of *Manta birostris* (Chondrichthyes: Mobulidae) in southeastern Brazil. *Ichthyological Research*, 56(1), 96–99. doi:10.1007/s10228-008-0060-3

Kim S.L., Casper D.R., Galván-Magaña F., Ochoa-Díaz R., Hernández-Aguilar S. B. & Koch P.L. 2012. Carbon and nitrogen discrimination factors for elasmobranch soft tissues based on a long-term controlled feeding study. *Environmental Biology of Fishes*, 95(1): 37-52.

Marshall, A. D., Compagno, L. J. V., & Bennett, M. B. 2009. Redescription of the genus *Manta* with resurrection of *Manta alfredi*. *Zootaxa*, 28, 1–28.

Marshall, A. D., & Bennett, M. B. 2010. Reproductive ecology of the reef manta ray *Manta alfredi* in southern Mozambique. *Journal of Fish Biology*, 77, 169–190. doi: 10.1111/j.1095-8649.2010.02669.x

- Marshall, A. D., Dudgeon, C. L., & Bennett, M. B. 2011. Size and structure of a photographically identified population of manta rays *Manta alfredi* in southern Mozambique. *Marine Biology*, 158, 1111–1124. doi: 10.1007/s00227-011-1634-6
- Martins, A. P. B., Heupel, M. R., Chin, A., & Simpfendorfer, C. A. 2018. Batoid nurseries: definition, use and importance. *Marine Ecology Progress Series*, 595, 253–267. doi: 10.3354/meps12545
- McCauley, D.J., DeSalles, P.A., Young, H. S., Papastamatiou, Y.P., Caselle, J.E., Deakos, M.H., et al. 2014. Reliance of mobile species on sensitive habitats: a case study of manta rays (*Manta alfredi*) and lagoons. *Marine Biology*, 161, 1987–1998. doi: 10.1007/s00227-014-2478-7
- Mendoça, S.A., Macena, B.C.L., Alfonso, A.S. & Hazin, F.H.V. 2018. Seasonal aggregation and diel activity by the sicklefin devil ray *Mobula tarapacana* off a small, equatorial outcrop of the Mid-Atlantic Ridge. *Journal of Fish Biology*, doi: 10.1111/jfb.13829
- Newsome SD, Clementz MT & Koch PL. 2010a. Using stable isotope biogeochemistry to study marine mammal ecology. *Marine Mammal Science*, 26: 509–572
- Newsome, S. D., Bentall, G. B., Tinker, M. T., Oftedal, O. T., Ralls, K., Estes, J. A. & Fogel, M. L. 2010b. Variation in $\delta^{13}\text{C}$ and $\delta^{15}\text{N}$ diet–vibrissae trophic discrimination factors in a wild population of California sea otters. *Ecological Applications*, 20: 1744–1752. doi:10.1890/09-1502.1
- Notarbartolo di Sciara, G. 1987. A revisionary study of the genus *Mobula* Rafinesque, 1810 (Chondrichthyes: Mobulidae) with the description of a new species. *Zoological Journal of the Linnean Society*, 91, 1–91. doi: 10.1111/j.1096-3642.1987.tb01723.x

- Notarbartolo di Sciara, G. 1988. Natural history of the rays of the genus *Mobula* in the Gulf of California. *Fishery Bulletin*, 86, 45–66.
- Obeso-Nieblas M, Gaviño-Rodríguez JH, Jiménez-Illescas AR, Shirasago-Germán B .2002. Simulación numérica de la circulación por marea y viento del noroeste y sur en la Bahía de La Paz, B.C.S. *Oceánides*, 11:1–2
- Parrng E, Crumpacker A & Kurle CM. 2014. Variation in the stable carbon and nitrogen isotope discrimination factors from diet to fur in four felid species held on different diets. *Journal of Mammalogy*, 95: 151–159
- Paulin CD, Habib G, Carey CL, Swanson PM & Voss GJ. 1982. New records of *Mobula japonica* and *Masturus lanceolatus*, and further records of *Luvaris imperialis*. *New Zealand Journal of Marine and Freshwater Research*, 16: 11–17.
- Porras-Peters, H., Aurióles-Gamboa, D., Cruz-Escalona & V.H., and Koch, P.L. 2008. Trophic level and overlap of sea lions (*Zalophus californianus*) in the Gulf of California, Mexico. *Marine Mammal Science*, 24(3): 554–576. doi:10.1111/j.1748-7692.2008.00197.x.
- Post D.M., Pace M.L & Hairston N.G. 2000. Ecosystem size determines food-chain length in lakes. *Nature*, 405(6790): 1047-1049.
- Post D.M. 2002. Using stable isotopes to estimate trophic position: models, methods, and assumptions. *Ecology*, 83(3): 703-718.
- Post D.M., Layman C.A., Arrington D.A., Takimoto G., Quattrochi J. & Montana C.G. 2007. Getting to the fat of the matter: models, methods and assumptions for dealing with lipids in stable isotope analyses. *Oecologia*, 152: 179–189.

- R Development Core Team (2018). R: A language and environment for statistical computing. R Foundation for Statistical Computing, Vienna, Austria. ISBN 3-900051-07-0, URL <http://www.R-project.org>.
- Rohner C, Pierce S, Marshall A, Weeks S, Bennett M & Richardson A. 2013. Trends in sightings and environmental influences on a coastal aggregation of manta rays and whale sharks. *Marine Ecology Progress Series*, 482: 153–168.
- Salomón-Aguilar CA, CJ Villavicencio-Garayzar & H Reyes-Bonilla. 2009. Shark breeding grounds and seasons in the Gulf of California: Fishery management and conservation strategy. *Ciencias Marinas*, 35(4): 369–388
- Sampson, L., Galván–Magaña, F., De Silva-Dávila, R., Aguiniga-Garcia, S., & O’Sullivan, J. B. 2010. Diet and trophic position of the devil rays *Mobula thurstoni* and *Mobula japanica* as inferred from stable isotope analysis. *Journal of the Marine Biological Association UK*, 90, 969–976. doi: 10.1017/S0025315410000548
- Santamaría-Del-Angel, E., Alvarez-Borrego, S., Millán-Nuñez, R. & Muller-Karger, F.E. 1999. Sobre el efecto de las surgencias de verano en la biomasa fitoplanctónica del Golfo de California. *Revista de la Sociedad Mexicana de Historia Natural*, 49, 207–212
- Simpfendorfer C. & Milward N. 1993. Utilization of a tropical bay as a nursery area by sharks of the families Carcharhinidae and Sphyrnidae. *Environmental Biology of Fishes*, 37: 337–345
- Smith, P.E. & Richardson, S.L. 1979. Técnicas modelo para prospecciones de huevos y larvas de peces pelágicos. FAO Documento Técnico de Pesca. No.175. Rome. FAO. 107p.

- Smith, W.D, Bizzarro, J.J & Cailliet, G.M. 2009. The artisanal elasmobranch fishery on the east coast of Baja California, Mexico: Characteristics and management considerations. *Ciencias Marinas*, 35(2): 209–236
- Snelson F.F., Mulligan T.J. & Williams S.E. 1984. Food habits, occurrence, and population structure of the bull shark, *Carcharhinus leucas*, in Florida coastal lagoons. *Bulletin of Marine Science*, 34: 71-80
- Stevens JD, Bonfil R, Dulvy NK & Walker PA. 2000. The effects of fishing on sharks, rays, and chimaeras (chondrichthyans), and the implications for marine ecosystems. *ICES Journal Marine Science*, 57: 476–494.
- Stevens, G. M. W. 2016. Conservation and Population Ecology of Manta Rays in the Maldives. PhD dissertation, University of York. York, UK.
- Stevens, G. M. W., Hawkins, J. P., & Roberts, C. M. 2018. Courtship and mating behaviour of manta rays *Mobula alfredi* and *M. birostris* in the Maldives. *Journal of Fish Biology*, doi: 10.1111/jfb.13768.
- Stewart, J. D., Rohner, C. A., Araujo, G., Avila, J., Fernando, D., Forsberg, K., et al. 2017. Trophic overlap in mobulid rays: insights from stable isotope analysis. *Marine Ecology Progress Series*, 580, 131–151. doi: 10.3354/meps12304
- Stewart Joshua D., Jaine Fabrice R. A., Armstrong Amelia J., Armstrong Asia O., Bennett Michael B., Burgess Katherine B., et al. 2018a. Research Priorities to Support Effective Manta and Devil Ray Conservation. *Frontiers in Marine Science*, vol: 5, 314. doi:10.3389/fmars.2018.00314
- Stewart, J. D., Nuttall, M., Hickerson, E. L., & Johnston, M. A., 2018b. Important juvenile manta ray habitat at flower garden banks national marine sanctuary in the northwestern Gulf of Mexico. *Marine Biology*, 165:111. doi: 10.1007/s00227-018-3364-5

- Tenzing P. 2014. The eco-physiology of two species of tropical stingrays in an era of climate change. PhD dissertation, James Cook University, Townsville.
- Trejo, A. 2017. Caracterización de la Bahía de La Paz, Baja California Sur, México, como una posible área de crianza del tiburón bironche, *Rhizoprionodon longurio* (Jordan & Gilbert, 1882). Master Science dissertation, Instituto Politécnico Nacional, México.
- Uchida, S., Toda, M., & Matsumoto, Y. 2008. Captive records of manta rays in Okinawa Churaumi Aquarium, in Joint Meeting of Ichthyologists and Herpetologists (Montreal, QC), 23–28.
- Vander-Zanden M.J. & Rasmussen J.B. 2001. Variation in $\delta^{15}\text{N}$ and $\delta^{13}\text{C}$ trophic fractionation: implications for aquatic food web studies. *Limnology and Oceanography*, 46(8): 2061-2066.
- Villavicencio-Garayzar, C.J. 1991. Observations on *Mobula munkiana* (Chondrichthyes: Mobulidae) in the Bahía de la Paz, B.C.S., Mexico. *Revista Investigaciones Científicas*, 2(2):78–81.
- VUE Software Manual, Version 2.5. 2014. Vemco, Bedford, Nova Scotia, Canada
- Ward-Paige CA, Davis B & Worm B. 2013. Global population trends and human use patterns of Manta and Mobula rays. *PLoS One*, 8:e74835.
- Wearmouth VJ & Sims DW. 2008. Sexual segregation in marine fish, reptiles, birds and mammals: behaviour patterns, mechanisms and conservation implications. *Advances in Marine Biology*, 54: 107–170.
- White W, Giles J & Potter I. 2006. Data on the bycatch fishery and reproductive biology of mobulid rays (Myliobatiformes) in Indonesia. *Fisheries Research*, 82: 65–73.

White ER, Myers MC, Flemming JM & Baum JK. 2015. Shifting elasmobranch community assemblage at Cocos Island an isolated marine protected area. *Conservation Biology*, 29:1186–1197.

Wourms, J. P. 1977. Reproduction and development in chondrichthyan fishes. *American Zoologist*, 17, 379–410.

Yokota L, Lessa RP. 2006. A nursery area for sharks and rays in Northeastern Brazil. *Environmental Biology of Fishes*, 75(3):349-60